VISCOELASTIC MODELING OF STRESS RELAXATION BEHAVIOR IN BIODEGRADABLE POLYMERS

By

VIJAYALAKSHMI SETHURAMAN

Bachelor of Technology in Chemical Engineering

Anna University

Chennai, Tamilnadu

2011

Submitted to the Faculty of the
Graduate College of the
Oklahoma State University
in partial fulfillment of
the requirements for
the Degree of
MASTER OF SCIENCE
May, 2013

VISCOELASTIC MODELING OF STRESS

RELAXATION BEHAVIOR IN BIODEGRADABLE

POLYMERS

Thesis Approved:

Dr. Sundar V. Madihally

Thesis Adviser

Dr. Arland H Johannes

Dr. R Russell Rhinehart

ACKNOWLEDGEMENTS

First I would like to thank my advisor Dr. Sundar Madihally for his continuous support and guidance throughout the project. His high energy and spirits especially when things don't work had made me to work through my project constantly and without his patience this thesis wouldn't have been possible. I also would like to thank him for guiding and providing financial support for me throughout my Master's program.

I would like to thank my committee members Dr. Arland Johannes and Dr. Rhinehart for their interest in my research work. Also I would like to extend my special thanks to Dr. Rhinehart for helping me with modeling and also his guidance throughout the program. I have always inspired Dr. Rhinehart for the kind of work he does and it was great working with him.

People in my research played an energetic role in supporting me through the project giving me ideas to make it better. I would like to be grateful to Jagdeep Podichetty, Abdu Khalf, Jimmy Walker, Carrie German and Kumar Singarapu for their support.

This would have not been possible without Upasana Manimegalai Sridhar who helped from day one to pursue my degree as my sister; I would like to extend my thankfulness for her. Also I would like to thank my brothers Anand Govindarajan, Kumar Singarapu and Suresh Kumar Jayaraman and my friends Vaishnavi Srinivasan, Shakthi Varman, Karuppayee PL, Supriya Varadarajan, Samyuktha Koteeswaran, Sunil Kumar,

Jeet Turakhia, Lakshmi Nagarajan, Dushyanthi Vivekanandan, Ram Kumar and Nikitha Reddy for their continuous support and fun that we had together during my days at OSU.

Last but not the least I would like to thank my parents Sethuraman and Parvathavardini for their complete support and encouragement. This would be incomplete without thanking my lovable brother Ramakrishnan Sethuraman and sister-in-law Manasee Krishnamoorthy for all the support, encouragement and love that they have given me.

Dedicated to my lovable parents Sethuraman and Parvathavardini

Name: VIJAYALAKSHMI SETHURAMAN

Date of Degree: MAY, 2013

Title of Study: VISCOELASTIC MODELING OF STRESS RELAXATION BEHAVIOR IN BIODEGRADABLE POLYMERS

Major Field: CHEMICAL ENGINEERING

Abstract:

Regenerating tissues using biodegradable structures onto which cells attach, populate, and synthesize new tissue or a whole organ has become more essential due to the scarcity in donor transplants. The biodegradable structures from various animal tissues such as skin, bladder, fat and intestine have seen clinical usage due to the advantage of premade architecture, which is conducive for tissue regeneration. However, manipulating these architectures to grow other tissues has shown many obstacles. Hence, synthesizing matrixes of both synthetic and natural polymers should possess bioactivity along with high porous structures to aid cell in-growth and mechanical strength to withstand the stresses and strains in the body. Biological tissues exhibit viscous (like fluids) and elastic (like solids) behavior, hence, prepared materials should have similar characteristics.

Previously we have reported on the stress relaxation characteristics of poly-lactic-co-glycolic acid (PLGA) films [1], polycaprolactone (PCL) films [2] and chitosan, chitosan-gelatin porous structures [3] formed by freeze-drying. We have also modeled some of the behavior using quasi-linear viscoelastic model and pseudo component models. The objective of this study was to evaluate and model the effect of processing scaffolds in viscoelastic behavior and also to compare the relaxation characteristics of polymers as different structures (scaffolds and films). For this purpose, we prepared PCL scaffolds by salt leaching technique and electrospun technique; chitosan, chitosan-gelatin films by air drying technique. First, uniaxial tensile properties were evaluated under physiological conditions (hydrated in phosphate buffered saline at 37 °C). From the estimated break strain, the limit of strain per ramp was calculated and stretched. The ramp-and-hold type of stress relaxation test was performed for five successive stages.

We developed two models using (i) 5- parameter model (containing two components with a hyper-elastic spring and suitable pseudo component) and (ii) 8-parameter model (containing three components with a hyper-elastic spring and two suitable pseudo components) in Visual Basic Applications accessed through MS Excel. The models were used to fit the experimental stress-relaxation data and parameters were obtained to understand the influence of porous architecture. To validate the utility of the models, obtained parameters were used to predict cyclic behaviors, which were compared independently with the cyclical experimental results. These results showed the model could be used to predict the cyclical behavior under the tested strain rates.

TABLE OF CONTENTS

Chapter Page

LIST OF TABLES

Table Page

LIST OF FIGURES

Figure Page

CHAPTER I

INTRODUCTION

Promising novel solutions to restore, maintain, enhance tissue function or a whole organ is regenerating tissues using biodegradable structures onto which cells attach, populate and synthesize new tissue. The biodegradable structures from various animal tissues such as skin, bladder, fat and intestine have seen clinical usage due to the advantage of premade architecture, which is conducive for tissue regeneration. However, manipulating these architectures to grow other tissues has shown many obstacles. Stem cells obtained from patient's soft and hard tissues can be extended in culture and planted on to scaffold structures which will slowly degrade and resorb as tissue structures suitable to be introduce in native environment. Whereas regeneration based on these techniques eliminate the problem of immune rejection, and donor site scarcity [1]. Scaffolds or three-dimensional (3-D) structures provides support for the cells to populate and defines the ultimate shape of a bone or a cartilage. Hence, synthesizing matrixes using various materials and processes such as electro spinning, freeze drying, 3D printing, and salt leaching techniques have been considered. Three dimensional scaffolds are prepared from both synthetic and natural materials that are i) compatible with the

human body, ii) bio-degradable and supportive of reparative cell- colonization using different natural and synthetic polymers has attracted significant interest [2]. In addition to showing bioactivity, scaffolds should have high porous structures to aid cell in growth and mechanically withstand the stresses and strains in the body. Biological tissues exhibit viscous (like fluids) and elastic (like solids) behavior, hence, the synthesized synthetic scaffolds which are used to replace the natural tissue for repair purposes need to possess viscoelastic properties compatible with the native environment [3]. Understanding the viscoelastic behavior of scaffold material becomes more significant in predicting its behavior for various applications. In order to analyze the viscoelastic behavior, two widely used material in tissue regeneration namely natural polymer chitosan and synthetic polymer polycaprolactone (PCL), were taken for study.

The objectives of the study is to

(i) *To understand the effect of scaffold preparation techniques on the viscoelastic behavior of synthetic polymer PCL*. For this purpose the PCL scaffolds of 45 kDa and 80 kDa MW were prepared using salt leaching technique [4] and electrospinning technique [5]. The scaffolds were characterized with scanning electron microscopy (SEM) analysis and pore architecture was established. Thickness of scaffolds, porosities and fiber sizes were calculated for salt leached scaffolds and electrospun scaffolds, respectively. First, uniaxial tensile properties were evaluated under physiological conditions (hydrated in phosphate buffered saline at 37 °C). From the estimated break strain, the limit of strain per ramp was calculated and stretched. The ramp-and-hold type of stress relaxation test was performed for five successive stages. As the maximum stress for each sample was different, reduced relaxation functions G(t) was plotted by normalizing the relaxation

portion of the data to the highest stress experienced by each structure in the first stage. G(t) plots were plotted for all five stages of each scaffolds, and also for first stage of all scaffolds together to compare the relaxation characteristics. Overall, PCL scaffolds by electrospun technique relaxes more than the scaffolds by salt leaching technique, however films relaxes more than that of scaffolds.

(ii) *To analyze the relaxation behavior of natural and synthetic polymer, and also to compare its behavior in different structures as scaffolds and films*. Previously we reported on the stress relaxation characteristics of PCL films [6] formed by air drying and chitosan, chitosan-gelatin porous structures formed by freeze-drying [7]. For this purpose a natural polymer chitosan, chitosan-gelatin films prepared by air drying technique was experimented under similar conditions as that of scaffolds. In case of PCL, the films were experimented under different set of conditions so the relaxation experiments were repeated under similar conditions as that of scaffolds on PCL films formed by air drying technique to compare its behavior. In chitosan scaffolds relaxes more than films and in PCL films relaxes more than scaffolds; however chitosan relaxes more than PCL.

(iii) *To investigate the model adaptation to the viscoelastic behavior to synthetic polymer scaffolds and to explore on the flexibility of pseudo component modeling on films.* Pseudo component modeling was developed with components (i) hyper-elastic spring (containing two parameters) (ii) spring and dashpot (containing three parameters) (iii) retain (containing three parameters) (iv) reform (containing three parameters) in Visual Basic Applications accessed through MS Excel [7]. 5- and 8- parameter models were used to fit the experimental stress-relaxation data and parameters were obtained to understand the influence of porous architecture of scaffolds. The combination of the

models were chosen based on the SEM analysis of the samples before and after the ramp and hold tests. For chitosan scaffolds the molecules were aligned in the direction of pull after the tests so the retain component of the model was chosen to fit the experimental data, whereas in PCL scaffolds only few molecules were aligned in the direction of pull, other molecules were randomly oriented so the reform component of the model was chosen to fit the experimental data. Two VBA macros were written which includes 5 parameter (hyper-elastic and retain component) and 8 parameter model (hyper-elastic, retain and retain component) to reduce the sum of squared deviation (SSD) between the experimental and modeled stress data. To validate the utility of the models, obtained parameters were used to predict cyclic behaviors, which were compared independently with the cyclical experimental results. These results showed the model could be used to predict the cyclical behavior under the tested strain rates.

Thus the viscoelastic nature of synthetic polymer (PCL) due to different processing techniques, molecular weight was analyzed. Also, the relaxation trends between natural and synthetic polymers, as different structures of the polymer such as films and scaffolds were compared. Pseudo component modeling was used in fitting the relaxation trends of chitosan and PCL scaffolds and films. Leapfrogging optimizer was employed in reducing the SSD between the experimental and modeled stress data. The modeled was validated using the parametric values from relaxation behavior to predict the cyclical behavior of scaffolds.

CHAPTER II

BACKGROUND

2.1. Tissue engineering

Tissue engineering technology has been developed to construct artificial tissues that can mimic the natural ones by combining modulated cells with different types of scaffolding materials, which are synthesized from various natural and synthetic polymers. These polymer scaffolds can be chemically modified to exhibit selective cell adhesion properties on many cell types including smooth muscle cells, endothelial cells, hepatocytes and chondrocytes, which enhance cell attachment and further growth of tissues [8]. Three-dimensional (3-D) scaffolds of biodegradable polymers are being popularly used for cell culture to regenerate tissue-based artificial organs [9]. The basic principle of tissue engineering (**Figure.2.1**) involves harvesting cells from the body of patient where the tissues are to be regenerated are populated using cell culture technique, and these cells are then fed on to the biodegradable scaffolds synthesized from natural and synthetic polymers. The cells are cultured to populate in these scaffolds using bioreactors and a graft suitable for native environment is generated and is introduced into the body. This type of tissue regeneration is called in vitro tissue regeneration.

When these cells are made to populate after they are being introduced into the native environment, is called in vivo tissue regeneration. However for both tissue regeneration techniques, the scaffold properties play a vital role in mimicking those natural tissues.

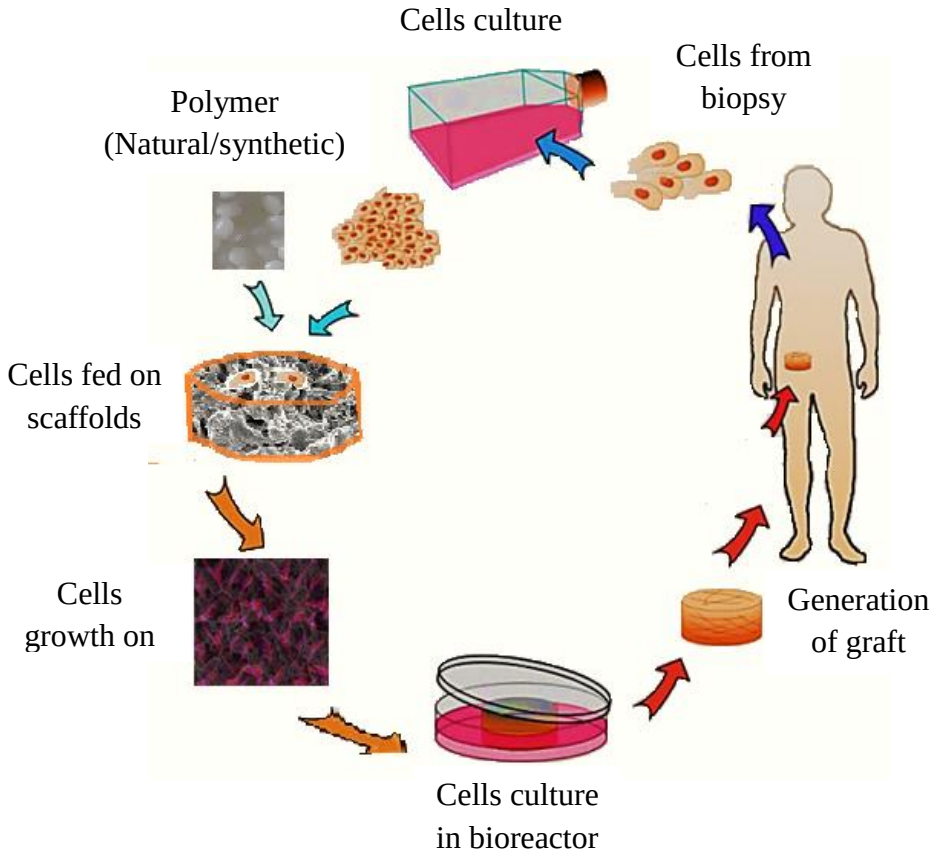

Figure 2.1. Basic principles of tissue engineering

The basic requirements of scaffolds include physical, chemical and mechanical factors suitable for tissue regeneration. Physical factors accounts for the porosity, pore size and topography of scaffolds with highly interconnected pore network suitable for cell growth and flow transport of nutrients and metabolic waste; chemical factors include the cell-material interaction property mainly for cell culture process where the scaffolds should be biocompatible, bioresorbable and resorption rate to match cell/tissue growth *in vitro*

and/or *in vivo* tissue regeneration; mechanical factors accounts for the strength, elasticity, degradation rate of the scaffolds.

2.2. Synthetic and natural polymers

Both natural and synthetic scaffolds provide a matrix onto which cells are fed for growth and regeneration. These approaches are used for cartilage replacement in the shape of a human ear; as tendons in orthopedic surgery, human urothelial and bladder muscle structures. The biocompatibility and biodegradability of these polymers are vital properties to be considered before implantation into the body [10].

2.2.1. Synthetic polymers

Synthetic polymers are attractive because they can be fabricated into various shapes with desired pore morphologic features conducive to tissue in-growth. The key advantages include the ability to tailor mechanical properties and degradation kinetics to suit various applications. Biodegradation is a natural process by which organic chemicals in the environment gets converted to simpler compounds and redistributed through elemental cycles such as carbon, nitrogen and sulfur cycles [11]. Biodegradable synthetic polymers includes polyesters like polycaprolactone, poly(vinyl alcohol), poly(vinyl acetate), poly(lactic-co-glycolic acid) and their copolymers which have been used in a number of clinical applications [12].

Poly (glycolic acid) (PGA) is polyester prepared by ring-opening polymerization of glycoside and its structure is $(O\text{-}CH_2\text{-}CO\text{-})_n$. It is a highly crystalline, rigid and biodegradable thermoplastic polymer. PGA is well suited for many biomedical

applications and it is commonly used as resorbable sutures. Porous scaffolds can be made using PGA but its properties and degradation rate varies depending on the processing technique used in synthesizing scaffolds [12].

Poly Lactic acid (PLA) is synthesized by the ring opening polymerization of lactide in the presence of metal catalysts. The PLA structure is $H-(O-\underset{\underset{CH_3}{|}}{\overset{\overset{H}{|}}{C}}-\overset{\overset{O}{||}}{C})_m-OH$. The main two monomers in the polymer is the lactic acid and cyclic di-ester lactide. Although structurally very similar to PGA, chemical, physical, and mechanical properties of PLA are different due to the presence of a pendant methyl group on the alpha carbon. Due to the presence of asymmetric carbon it makes the polymer to be a chiral molecule and so it has forms of L, D, and DL isomers. Poly(L-lactide) (PLLA) is a semi crystalline and relatively hard materials with glass transition temperature at about 65°C and melting temperature of about 170–180°C.

Co-polymerization of PGA with PLA reduces the degree of crystallinity and increases the rate of hydration and hydrolysis. The degradation rate depends on the ratio of the monomers used in copolymer synthesis [13]. So porous scaffolds by combining PLA-PGA have been synthesized and have been reported for many successful tissue repair processes. Concerns about PLA-PGA includes the release of toxic solutions with high local acid concentrations and also causes inflammatory response when it release small particles during degradation[12]. The degradation properties of a scaffold are essential for biomaterial selection.

Polycaprolactone (PCL) is biodegradable polyester synthesized by the ring-opening of the cyclic monomer ε- caprolactone. Its structure is $-(O-(CH_2)_5-\overset{\overset{O}{||}}{C})-$. PCL is non-

toxic, inexpensive and hydrophobic in nature with low melting point (60°C) attributing to its high solubility nature. It is a semi-crystalline polymer and its crystallinity decreases with increase in molecular weight. Physico-mechanical properties of PCL which includes its thermal properties (T_g, crystallization, melting and decomposition points), tensile properties including tensile strength, elongation at yield and at break have been investigated. Applications of PCL scaffolds include tissue engineered skin substitutes and also for controlled drug release by blending with PLA and cellulose acetate [14]. PCL films has been used as dressing cutaneous wounds and also used as a release vehicle for the chemical antiseptic chlorohexidine. PCL lacks bioactivity i.e., the cells are not stimulated by any specific interactions so that they can grow or differentiate in to a type of cells. In order to overcome this PCL has been blended with other molecules for specific applications [15]. As PCL can be processed using different techniques with a wide range of biomedical application and relatively inexpensive, it has been explored in this project.

2.2.2. Natural polymers

Natural polymers are those occurring in nature formed by complex metabolic process during the growth cycles of all organisms. These polymers are secreted by cells and gets assembled outside; their synthesis involves enzyme-catalyzed, chain growth polymerization reactions [11]. Many matrix components present outside the cells are known to play a significant role in tissue remodeling. Natural polymers have the advantage of exposure to the intrinsic properties of cell recognition due to resemblance to extracellular matrix materials and they are hydrophilic in nature. Some common natural

polymers include starch, cellulose, chitin, chitosan, collagen, and gelatin.

Chitosan is partially deacetylated from naturally occurring chitin which is a primary structural polymer in exoskeleton. Chitosan is a crystalline polymer which is soluble in acidic solutions (pH < 7) [15]. Its structure is represented by

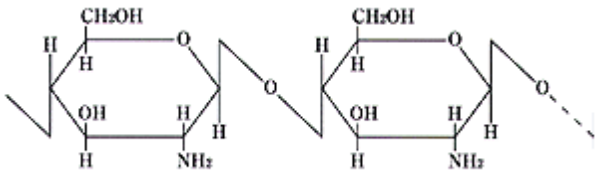

Chitosan has drawn attention due to its low cost, easy availability, positive charge, anti-microbial activity, and biocompatibility. It could be easily processed into films and scaffolds for biomedical applications which includes wound dressings, drug delivery systems, as space filling implants [16], articular cartilage, intervertebral disk and in bone tissue engineering [17]. Since chitosan is derived from chitin, there exists limitation on tailoring mechanical properties, flexibility and degradation. In the regenerative process, these scaffolds not only provide three-dimensional frameworks to form the designed tissues, but also fills space and controlled release of signals [18].

Gelatin is obtained from fibrous insoluble protein collagen, which is a major component of skin, bone, and connective tissue. Gelatin is inexpensive, nonirritating, biocompatible, and biodegradable. It has a long history of safe use in pharmaceuticals, cosmetics, as well as food products, and adhesives in clinics [19]. It is considered as ‘‘generally regarded as safe (GRAS)’’ material by the United States Food and Drug Administration. Gelatin promotes cell adhesion and growth. Gelatin has antigenicity (ability of a chemical structure to bind specifically with a group of certain products that have adaptive immunity), and restorability [20]. Gelatin as hydrogel porous structures is used for a

unique feature in medical field, such as nerve regeneration. The inner porous structure synthesized by varying the freeze-drying conditions can produce scaffolds with mass diffusion control and can be fabricated which is a crucial factor in using bioreactors for cell growth [21]. However, weak mechanical strength and inadequate tailor ability to alter mechanical and degradation properties limits its usage. Hence, gelatin in combination with chitosan and PCL is more popularly used than gelatin alone. Blending other polymers is based on improving the mechanical strength of gelatin. Chitosan-gelatin scaffolds are widely explored in a wide variety of tissue regeneration application; PCL-gelatin scaffolds are explored in bone regeneration [22]. Chitosan and gelatin have been extensively studied in our research group so it was chosen to compare the effect of natural and synthetic polymer relaxation characteristics.

2.3. Processing technique for scaffold formation

Porous scaffolds are used in tissue engineering as temporary structures to guide the growth of cells and regenerating tissues. Hence they are biodegradable and often involve compounds which have been already approved for human implantation [16]. Initial development and fabrication of scaffolds has spawned wide applications from industry to biomedical sciences. Extrusion, calendaring, and blowing are the common industrial methods for fabricating polymer sheets and thin films of thickness ranging from tens to hundreds of micrometers. These methods usually produce moderate level of chain orientation and are only suitable for low to moderate load-bearing applications. However, such limitation can be overcome by physically drawing the films to give

thinner films and at the same time improve the tensile strength and modulus because of the induced orientation of the fibrils [23].

Recent development are centered on forming porous scaffolds of various sized and shapes using various techniques including particulate leaching, salt leaching, electro spinning, sintering, freeze-drying, three-dimensional printing technique, gas forming techniques [24]. Few techniques are described below.

2.3.1. Salt leaching technique

This method of polymer scaffold preparation utilizes initial casting into required shape and leaching the porogen out of the cast. First, the polymer is dissolved in appropriate solvent to obtain a homogeneous solution. Then porogen such as sodium chloride (NaCl) salt crystals, which do not dissolve in the solvent used for dissolving polymer, are added to the polymer solution [4]. These porogens are pulverized using a mortar and pestle to get a required size, as the size of salt crystals determine the pore size of scaffolds. The paste of polymer containing the porogen is poured into a mold of required shape and the solvent is evaporated, typically by air drying. The solid polymer-porogen composite is then immersed in a solvent that selectively dissolves the porogen. For example, when NaCl is used, polymer-porogen composite is immersed in water for an extended period of time to dissolve the NaCl. Once the porogen is leached out, a porous scaffold of required shape is obtained. One concern with this method is ensuring inter-pore openings at low porosities where polymer solution could capsule the porogen.

2.3.2. Freeze drying

This method is more suitable when polymer solutions are water-based, although it can used in solvents which show a low melting point [25]. Formed polymer solutions are transferred into a mold of required shape. Then they are kept at appropriate temperatures to introduce a phase transformation in the solvent from liquid to solid. When water is the solvent, solution is frozen so that ice crystals are developed in the solution. Using aqueous polymer solutions, it has been shown that freezing temperature determines the size of the pores. These structures are sublimated to remove the crystals via vapor phase so that there is no structural collapse. The locations where crystals were present will become pores [26]. Main advantage of this technique is that, it neither requires high temperature nor separate leaching step. However it has the disadvantage of difficulty in precise control of pore size.

2.3.3. Phase Separation

Multicomponent polymer solution under certain conditions gets separated into polymer-rich and polymer lean phase. When the solvent is removed from polymer rich phase it solidifies to form the scaffolds.

Solid –Liquid phase separation: In polymer rich phase the solvent is removed by lowering the temperature thereby inducing the solvent to form crystals. When the solvent crystals are removed, the space occupied by the crystals becomes the pores with open arrays and microtubules. These oriented tubular scaffolds has anisotropic mechanical properties similar to tubular tissues like nerves, tendon, dentin and has been shown to facilitate cell organization into orientated tissues.

Liquid-liquid phase separation: In order to remove the solvent as the temperature is reduced sometimes it induces liquid-liquid phase separation of a polymer solution with an upper critical solution temperature. This leads to formation of bi-continuous structure of scaffolds with open-pore structure after the removal of solvent [27]. Scaffolds by this technique have the pore diameters ranging from a few to tens of microns and are often not uniformly distributed. So it is not well suitable for tissue engineering applications.

2.3.4. Electrospinning

Electrospinning can produce non-woven fibers of diameters ranging from nanometers to micrometer. By choosing a suitable polymer and appropriate solvent system, fiber size can be controlled (40 nm to 10 μm). Since the technology allows the possibility of tailoring the biomechanical properties, there has been a significant effort to adapt the technology in tissue regeneration [28]. Electrospinning technique requires three major components: a high voltage power supply, a spinneret and a collecting plate. The polymer solution is fed into the spinneret, when the voltage is applied electric field is developed between the spinneret and the collector plate. During which the surface tension of the droplet formed with the polymer solution is in equilibrium with the electric field. When the surface tension force overcomes the applied electric field force the droplet gets spun around as a fiber in the collector plate, during which the solvent evaporates. The resulting product is non-woven fibrous scaffolds [29]. Scaffolds from electrospinning provide a large surface area-to-volume ratio, highly interconnected pores with nanoscale fiber diameters which are similar to the extracellular matrices seen in living organisms. These properties, coupled with the fact that PCL is nontoxic and

inexpensive, make the material an advantageous choice for use in biomedical applications [30]. The fiber thickness and morphology can be controlled by various parameters that we use in the technique which includes viscosity, elasticity, conductivity and surface tension of the polymer solution, distance between the spinneret and the collecting plate, electric field strength.

2.4. Mechanical properties:

All scaffolds that are implanted into the body should possess mechanical properties that will retain its structure, in particular for the reconstruction of load bearing tissues like cartilages and bones. The bio stability of the implants depends on strength, elasticity, absorption at the material interface and chemical degradation [31]. By understanding the response of mechanical properties on porosity, pore size and degree of degradation we can design the biodegradable scaffolds suitable for tissue regeneration. Typical mechanical properties of the scaffolds are tested in uniaxial tension or compression. A perfectly elastic material stores all the energy created by the deformation forces so that on the removal of the forces, material can return to its original dimensions independent of time. Plastic material are those which don't comes back to the original structure even after the removal of applied strain it gets deformed. Popular biodegradable polyesters PGA, PLA and PLGA undergo plastic deformation and failure when exposed to long-term cyclic strains, limiting their use in tissue engineering [32]. However, majority of the tissues [33] and extracellular matrix elements in the body behave as viscoelastic materials rather than pure elastic materials [34]. Hence, understanding viscoelastic characteristics of scaffolds gains significance.

2.4.1. Viscoelastic behavior

Viscoelastic materials store and dissipate energy within the complex molecular structure, producing hysteresis and allowing creep during loading and unloading. A linear viscoelastic material could be a combination of obeying Newtonian viscous fluid characteristics while following Hook's law of linear elasticity. These materials return to their original structures following a different path to get back to original structure. There are materials whose response to a deforming load combines both viscous and elastic qualities; this property is called *viscoelasticity*.

Biological tissues display complex viscoelastic behavior which depends on the time and load-history of the tissues. Many soft tissues are extensively investigated to understand various disease mechanisms and injuries [35-38]. These results suggest that they show viscoelastic behavior under physiologic loading. Viscoelastic behavior is demonstrated either by fixed extension to the tissue, with the result that the initial stress generated decreases with time (stress relaxation) or by the application of a fixed stress, where upon the initial extension in the tissue fibers within a viscous matrix [39].

The viscoelastic properties of tissues create an environment for the cells which is critical for their viability and function. When a tissue is being replaced by a synthetic scaffold for repair, these tissues need to possess compatible viscoelastic properties as the native environment [30]. Understanding the viscoelastic behavior of the scaffold material is necessary in predicting how it performs during various applications. Although there are very few studies evaluating the viscoelastic properties of the synthetic scaffolds [6, 7], there have been many studies to understand the viscoelastic properties of the soft tissues [40-44]. Many models have also been proposed.

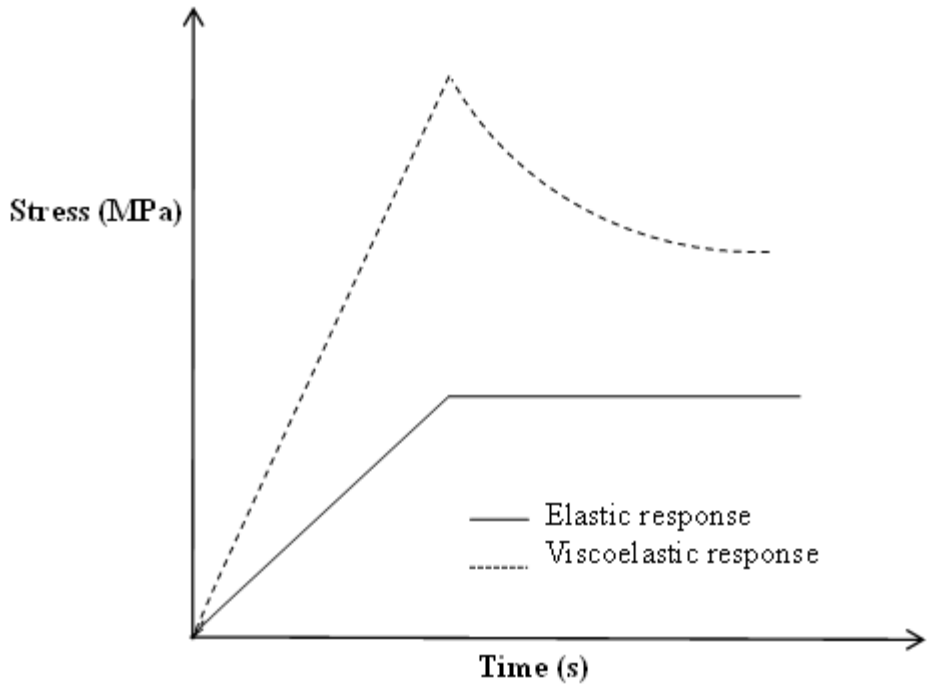

Figure 2.2. Stress-strain behavior of Elastic and Viscoelastic Materials

2.4.2. Viscoelastic models

All constitutive models are an approximation of the actual mechanical behavior of the tissue of interest. Most soft tissues exhibit a nonlinear viscoelastic response to strain, beginning with an initial, soft ‘‘toe region’’ that is followed by a progressively stiffer ‘‘loading region’’. Depending on the application, certain approximations may justify the use of a simpler or different constitutive model. A linear model is only accurate near the reference strain used in the model, and will not be accurate for strains even a few percent greater or less than the reference strain, hence, nonlinear models are preferred [45]. Various models used in tissue mechanics are tabulated in **Table 2.1,** giving examples of their application and limitations.

Standard linear solid (SLS) model: Few viscoelastic models have been proposed for relaxation characteristics of polymer. For example, standard linear solid (SLS) model has been used to describe behavior of PEG matrixes. The elements in the SLS model includes a spring (equilibrium arm) arranged in parallel with a spring and dashpot in series (Maxwell arm). SLS model represents the cumulative elemental contribution in response to tissue-material interaction. By incorporating the PEG: dextran(aldehyde) composition information into model, a design tool for adjusting material composition suitable for an application was described in a recent report [46]. They showed that the concentration of aldehydes determined the extent of internal and external adhesion to tissue, and at critical PEG: dextran (aldehyde) composition increasing the aldehyde concentration reduced the external adhesion to tissues. The authors state that incorporating steric effects into the model is necessary for other clinical applications where further adjustments are required in the composition.

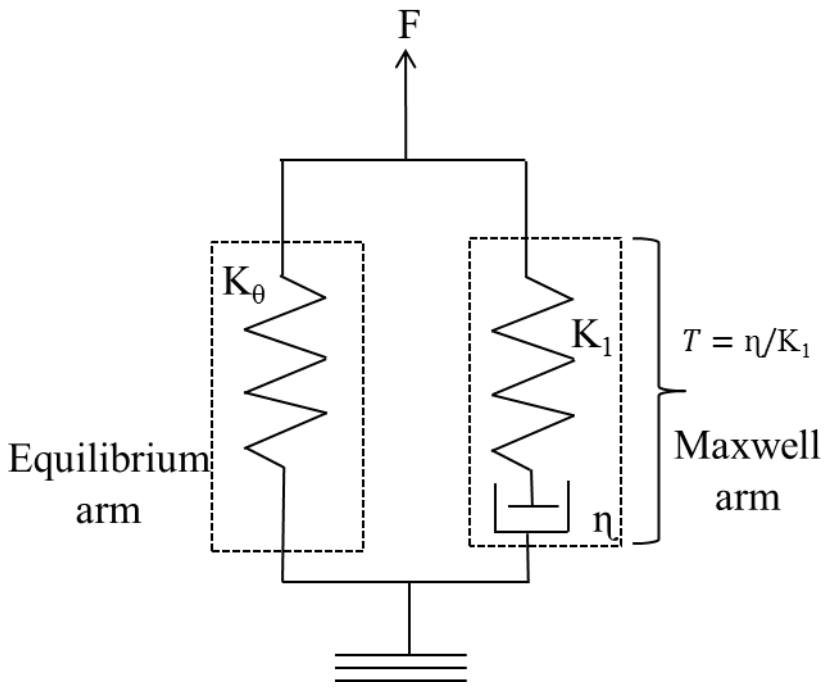

Figure 2.3.Schematic representation of Standard linear solid (SLS) model

Quasi-linear viscoelasticity: For many nonlinear viscoelastic behaviors of biological tissues modeling is done using Fung's theory of quasi-linear viscoelasticity (QLV). Fung's QLV theory assumes that a material's response can be separated into strain-dependent and time-dependent components. The bases for this theory are (i) the stress at a given time can be described by separating the elastic response and relaxation function, and (ii) that the relaxation functions has a continuous spectrum. Advantage of QLV model is that it is simpler than nonlinear but more accurate than linear model, and suitable for computer models that allow nonlinear spring and dashpot functions [45]. QLV has continued to remain a valuable tool in the field of biomechanics for analyses of various tissues including cartilage, ligaments, muscle and bone[47]. QLV models, however, suffer from many limitations including inability to model non stationary behavior, and confounding aspects of biological tissues structures [41, 48, 49]. Although QLV model is better in describing nonlinear behavior it cannot describe repetitive viscoelastic behavior and more general formulations are required.

Quasi-linear power law adaptation model: This model is constructed to predict both the power-law stress relaxation and quasi-linear viscoelasticity in lung tissues. This model has a Maxwell's arm which has a non-linear spring with dashpot in parallel fashion. It is advantageous over other conventional models (i) as it exhibits power law stress relaxation without requiring a special distribution of constitutive properties among its elements (the elements are all identical), and (ii) it automatically exhibits quasi-linear viscoelastic behavior, in both qualitative and quantitative agreement with experimental data. This

model predicts the rheology in unidirectional length, but lung tissues also exhibit stress-strain hysteresis and non-linearity which cannot be predicted with this model [50].

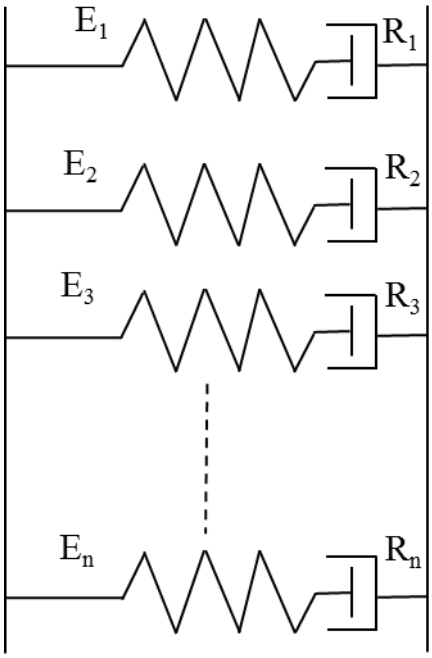

Figure 2.4. Schematic representation of Quasi-linear power law adaptation model

Helmholtz free energy density function model: Most recent approach in viscoelastic modeling is based on the Helmholtz free energy density function as the sum of a hyper-elastic term and a viscous term. By decomposing the stress tensor into initial and non-equilibrium parts, assuming the structure to be free energy density function that generalizes Kelvin–Voigt nonlinear viscous models. The stress tensor expresses the sum of elastic and dissipative component which is considered in developing the viscoelastic model [51]. This model is advantageous due to the ease in incorporating the resulting finite strain formulation into finite element code. The limitation of this model includes evaluating elevated number of parameters and also this model is related to QLV model formulation, it is restricted to small perturbations from equilibrium [52].

Table 2.1. Comparison of models used in predicting viscoelastic behavior.

Models	Applications	Limitations
Standard linear solid (SLS) model	Stress relaxation of PEG: dextran adhesives used for wound healing of intestinal tissues.	Depends mainly on the concentration of PEG: dextran, doesn't work at critical concentrations.
Quasi linear power-law adaption model	Characterizing lung tissue	Predicts only in unidirectional length doesn't capture the non-linearity completely.
Quasi-linear viscoelasticity.	Biological tissue behavior, human periodontal ligament	Can't describe all non-linearity in the system
Finite elemental modeling	Mechanical response for functional units of spine with varying external loads	Doesn't include fluid movement in spines.
Modified finite element modeling	Medial collateral ligament in knee	Doesn't represent the fluid phase in soft tissues.
Helmholtz free energy density function model	Ligaments response on large deformation	Restricted to small perturbations from equilibrium
Pseudo component modeling	Modeling soft tissues	More number of parameters to evaluate

Finite elemental modeling: Finite element analysis explains the solid and structural mechanics (bone mechanics included). These are converted with respect to computational modeling tools, as it can provide the ability to estimate with good accuracy how an object with a complex geometrical shape (*e.g.*, a whole bone or trabecular network) behaves when it is subjected to external loads. For predicting the relaxation characteristics in functional units of spine the model used in simulation consists of linear elastic solid, viscoelastic solid, nonlinear spring and dashpot. The methodology used was to identify the time dependent (viscoelastic) material in each segment and their response was evaluated using experimental analysis. The simulation results of the response of final model with the optimized set of parameters. It continuously changes model parameters to get least R^2 value in regression; instead analyzing the material response for individual elements can give more accurate results. When this model is used to predict the mechanical behavior in spine, there is greater influence of fluid movements which include osmotic and swelling pressures and this model doesn't account for fluid movements [53].

Modified finite element model: In modeling behavior of ligaments and tendons, application of initial tension to finite element models, to simulate the initial stresses found in in vivo. Four steps are involved in developing the model

(i) create a transversely isotropic model to represent the material behavior of ligaments and tendons

(ii) develop a method to apply an initial stretch to finite element models using the material model

(iii) extend the material model to viscoelasticity and

(iv) develop a finite element implementation of the material model.

The constitutive models are implemented into the nonlinear finite element codes NIKE3D and DYNA3D. The finite element implementation is efficient and robust, allowing for the large scale modeling of in compressible visco-hyperelastic material behavior [54]. This model also doesn't represent the fluid phase in soft tissues.

Pseudo component modeling: As the classical viscoelastic models such as Maxwell's, Kelvin-Voigt, and Standard-Linear models are inadequate, and much effort has been focused on developing mathematical models that would be able to explain the stress-strain behavior of biological materials. Pseudo component modeling was developed for characterizing the viscoelastic behavior in scaffolds with components of hyperelastic spring, dashpot, retain and reform. 'The model accounts for:

(i) the stress-relaxation with time under a constant strain rate

(ii) the deformation of the material shape under constant load

(iii) the gradual return of the material to its original form once the load is released and

(iv) their inconsistent tissue properties' [7].

This modeling approach uses spring-and-dashpot based constitutive models, modified by including nonlinear hyper-elastic "spring" elements. Since many synthetic structures may not relax fully to the original internal structure in the first cycle, the commonly employed dashpot element (which lets the spring return to zero stress) is inappropriate. One of the major benefits of this model is that it takes into account the orientation of materials under loading conditions and chooses the components for constituting the

multi-component model. Limitation of this model is that it doesn't account for the internal tearing, elongation of voids and experimental vagaries. Our approach is to write the codes in Visual Basic Applications (VBA) through MS Excel and share as an open source with others. Every modeling technique has its advantages and limitations, for this study I have chosen pseudo component modeling approach as it characterizes the material after loading conditions.

CHAPTER III

POLYCAPROLACTONE SCAFFOLD ANALYSIS

3.1. Polycaprolactone Scaffold Processing

Polycaprolactone (PCL) is a synthetic biodegradable polymer with low melting point and adjustable mechanical properties. Scaffolds have been generated using PCL by various additive techniques such as electrospinning[5], rapid prototyping [55] and subtractive techniques such as salt leaching [4], and freeze drying [56]. The primary modes of mechanical property evaluation of these scaffold preparations are linear tensile and compression tests. Since natural tissues are viscoelastic, understanding the viscoelastic behavior of the scaffold material is necessary to predict its performs during various applications[30]. Though there have been many studies to understand the viscoelastic properties of the soft tissues the effect of different scaffold preparation techniques on viscoelastic properties is not well understood. The objective of this study was to understand the effect of scaffold preparation techniques on the viscoelastic properties of low and high MW PCL. The scaffolds of 45 kDa and 80 kDa MW were prepared using salt leaching technique [57] and electrospinning technique [58]. The effect of processing of these scaffolds in relaxation property was investigated. These results show significant effect of scaffold processing on stress relaxation characteristics.

3.2. MATERIALS AND METHODS

3.2.1. Materials

PCL of molecular weight 80,000 Da (referred as 80 kDa) was purchased from Sigma (St Louis, MO), PCL of molecular weight 43,000-50,000 Da (referred as 45 kDa) was purchased from polysciences Inc (Warrington PA), chloroform,1:2 from pharmco (Brookfield, CT) and phosphate buffer salts (sodium chloride, potassium chloride, potassium dihydrogen phosphate, sodium monohydrate phosphate heptahydrate) was purchased from Sigma-Aldrich (St Louis, MO).All chemicals were used as received without further purification.

3.2.2. Generation of scaffold by salt-leaching technique

Solutions were prepared at room temperature and stirred for 24 hours until the solutions became homogeneous. Scaffolds were prepared by salt-leaching technique using a previously published procedure [4]. In brief, sodium chloride salt crystals were pulverized using a mortar and pestle. These crystals were sieved using two trays (i) >274 µm sieve size and (ii) <246 µm sieve size to obtain crystals in the size of 246-274 µm. Then, 2.7 g of PCL was dissolved in 20 mL of chloroform (moisture content < 0.001%) and 29 g of 246-274 µm salt crystals was added to the solution to form a homogeneous paste. The paste was spread in 5 ×5 cm rectangular wells prepared on Teflon sheets using silicone glue and air dried in a laminar hood. Formed structure was immersed in distilled water for 20 hours to dissolve the salt and then analyzed by scanning electron microscopy to determine its pore architecture.

3.2.3. Generation of scaffolds by electrospinning technique

Scaffolds were prepared by electrospinning using our previously published procedure[59] with minor modifications. In brief, the electrospinning setup consisted of one syringe pump (74900 series, Cole-Parmer Instrument Company, Vernon Hills, IL), 10 mL syringe (Luer-Lok Tip; Becton Dickinson and Company, Franklin Lakes, NJ), needle tips, high voltage power supply (ES30P-5W/DAM, Gamma high Voltage Research, Ormond Beach, FL), earth grounding and a collection mandrel. Approximately 30 cm long PTFE tubing (Sigma Aldrich, St. Louis, MO) connected the syringe to the spinneret. 20%wt/v PCL solution in Methanol/Chloroform (1:2) was loaded into the syringe. A 12kV voltage was applied between the needle and the conductive collector. PCL spinning solution was pumped to the spinneret (0.8 mm inside diameter) at flow rate of 2 mL/h. Randomly distributed fibers were collected on a flat collector plate at a spinning distance of 10 cm. The collected fibers were then analyzed by SEM for fiber size and distribution.

3.2.4. Generation of films

PCL solution used for scaffold generation was air dried under laminar hood for 2 hours to form the films. Similar to scaffolds, 5 mL of the solution was poured into the rectangular well which was prepared using silicone glue on Teflon sheets. Since films formed by evaporating 5 mL of the solution were less elastic, solution quantity was reduced to 2 mL to obtain thinner films.

3.2.5. Microstructure characterization

Samples were analyzed using SEM similar to our previous publication[5]. In brief, samples were attached to an aluminum stub using a conductive graphite glue (Ted Pella Inc., Redding, CA) and sputter-coated with gold for 1 min. Samples were characterized JOEL 6360 (Joel USA Inc., Peabody, MA) SEM at an accelerated voltage of 15kV.

3.2.6. Determining structure thickness, pore size and fiber size

Thickness of salt leached and electrospun scaffold was measured using a digital caliper (Fisher Scientific). Film thickness was determined similar to previous publications, [60] where the films were cut into strips and oriented orthogonally in the field of view of the inverted microscope equipped with a CCD camera so as to measure the thickness. Digital micrographs were obtained at various locations and quantified using Sigma Scan Pro image analysis software (SPSS Science, Chicago, IL) for the thickness. At least 3 to 4 images were analyzed per sample, the calculated film thicknesses of 3 samples was used for determining the stress values during tensile testing.

Porosity of salt leached scaffolds was determined by cutting a thin strip of the samples adjacent to that used for testing. The cut strips were mounted to see the cross section and digital micrographs were obtained at various locations using an inverted microscope. Then the net area of the pores was calculated using Sigma Scan Pro image analysis software. Assuming isotropic distribution of pores throughout the scaffolds, porosity was calculated as the ratio of open pore area to the total image size. At least 3 to 4 images were analyzed per sample, to calculate the porosity of the scaffolds. The fiber diameters

in electrospun scaffolds were calculated using the micrographs acquired using SEM and Sigma Scan Proimage analysis software.

3.2.7. Mechanical testing

All tests were conducted in a physiological conditions (phosphate buffer solution at pH 7.4 at 37^0C) using INSTRON 5542 machine (INSTRON, Canton, MA) and a custom-built environmental chamber. The scaffolds and films were cut into dimensions of 50 mm long and 10 mm wide. Each test was performed 3 or more times using samples from different preparations.

Tensile tests: Samples were pulled at a cross head was set to 10 mm/min (0.17 mm/s) to break, similar to previous reports [7]. Break stress and strain were determined using the associated software, Merlin (INSTRON Canton, MA).

Stress- relaxation tests: Since salt leached scaffolds had lower break stress and strain limits (**Table 3.1**), the upper limit of total strain was set to 10% strain. Hence, the samples were stretched at a strain rate of 1% $s^{-1}$for 2 seconds in each stage which was repeated for 5 stages accumulating to 10% strain for entire experiment. Although the films had a different strain rate before its failure, in order to compare the stress relaxation behavior of films and scaffolds the strain rate of 1% s^{-1} was maintained for both films and scaffolds. Five stages of ramp and hold experiment were performed on different structures with a constant strain rate of 1%$s^{-1}$for 2 s (ramp) followed by 58 s relaxation (hold). At least three samples from different preparations were analyzed by each method. Averages stress values and relaxation function values were determined along with the standard deviation. Obtained relaxation behaviors were analyzed using three types of

graphical representations:

(i) comparing the absolute values of stresses at different times for different samples.

(ii) changes in stress in each stage was normalized to the origin and different stages for that sample were plotted on the same graph.

(iii) relaxation function, G(t), was plotted for the first stage by normalizing the relaxation data by the highest stress in that stage.

3.3. RESULTS

3.3.1. Characteristics of scaffolds

Obtained structure thicknesses for different structures (**Table 3.1**) were compared between the scaffolds prepared by salt leaching and electrospinning technique. Generally, high MW structures were thicker than low MW structures in both films and scaffolds. Microstructures of formed scaffolds were characterized to better understand the observed mechanical properties. These results showed (**Figure 3.1**) that the electrospun scaffolds had uniform micro size fibers with random orientation. The fiber thickness of the 80 kDa electrospun PCL scaffolds was 0.05 (±0.02) mm. There were no beads (small lumps due to salt leaching technique) in any part of the structure. When salt leached scaffolds were evaluated, both 45 kDa and 80 kDa scaffolds showed distribution of pores throughout the scaffold. The pores appeared interconnected.

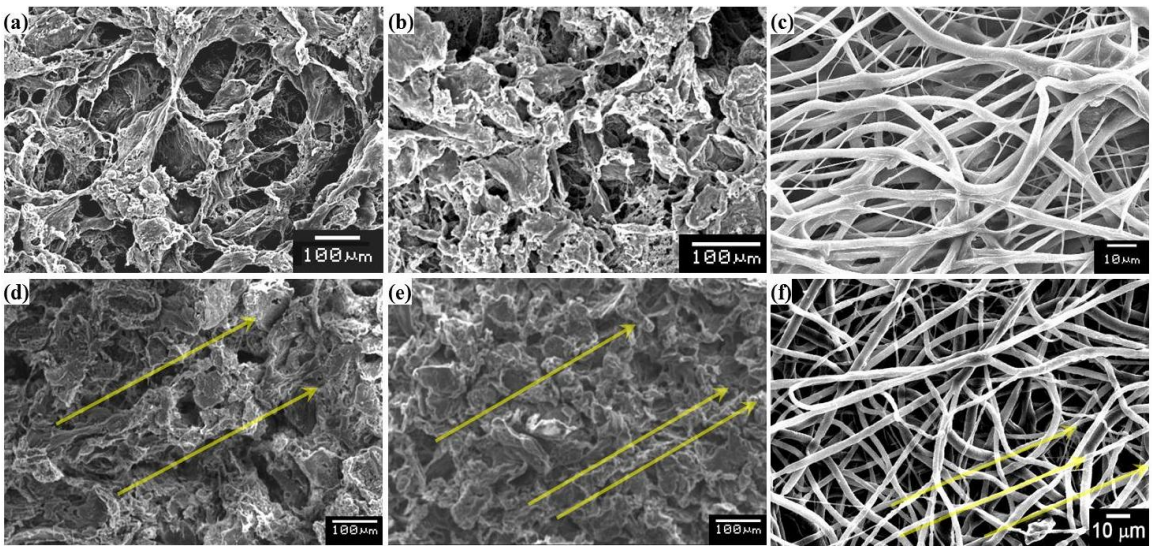

Figure 3.1. Micrographs of scaffolds showing porous structure before and after stress relaxation experiment. (a) 45 kDa salt leached (SL) scaffolds before stretching, (b) 80 kDa SL scaffolds before stretching, (c) 80 kDa electrospun scaffolds before stretching, (d) 45 kDa SL scaffolds after stretching, (e) 80 kDa SL scaffolds after stretching, (f) 80 kDa electrospun scaffolds after stretching.

3.3.2. Tensile testing

Uniaxial tensile testing results show (**Figure 3.2**) that the scaffolds had non-linear behavior even with small strain rate. Break stress and break strain was lowest for the 45 kDa scaffolds prepared by salt leaching technique followed by 80 kDa scaffolds prepared by salt leaching technique (**Table 3.1**). 80 kDa scaffolds by electrospun technique stretched more than salt leached scaffolds. Increased thickness of the electrospun scaffolds decreased the break strain. These values were significantly lower than that of 80 kDa films that we previously reported [6]. In general high MW structures showed higher break strain than low MW structures which is attributed to the chain length of the polymer.

Table 3. 1. Scaffold Characteristics

	Thickness (mm)	Porosity	Break Strain (%)	Break Stress (MPa)
Salt leached 45 kDa scaffolds	2.10 ±0.03	81.7±1.50	20-25	0.07
Salt leached 80 kDa scaffolds	2.17 ±0.03	82.6±1.20	25-30	0.08
Electrospun 80 kDa scaffolds	0.173 ±0.045	-	150-160%	1.5
45 kDa films	0.124 ±0.05		200-300	8
80 kDa films	0.129 ±0.04		>700 [6]	~12 [6]

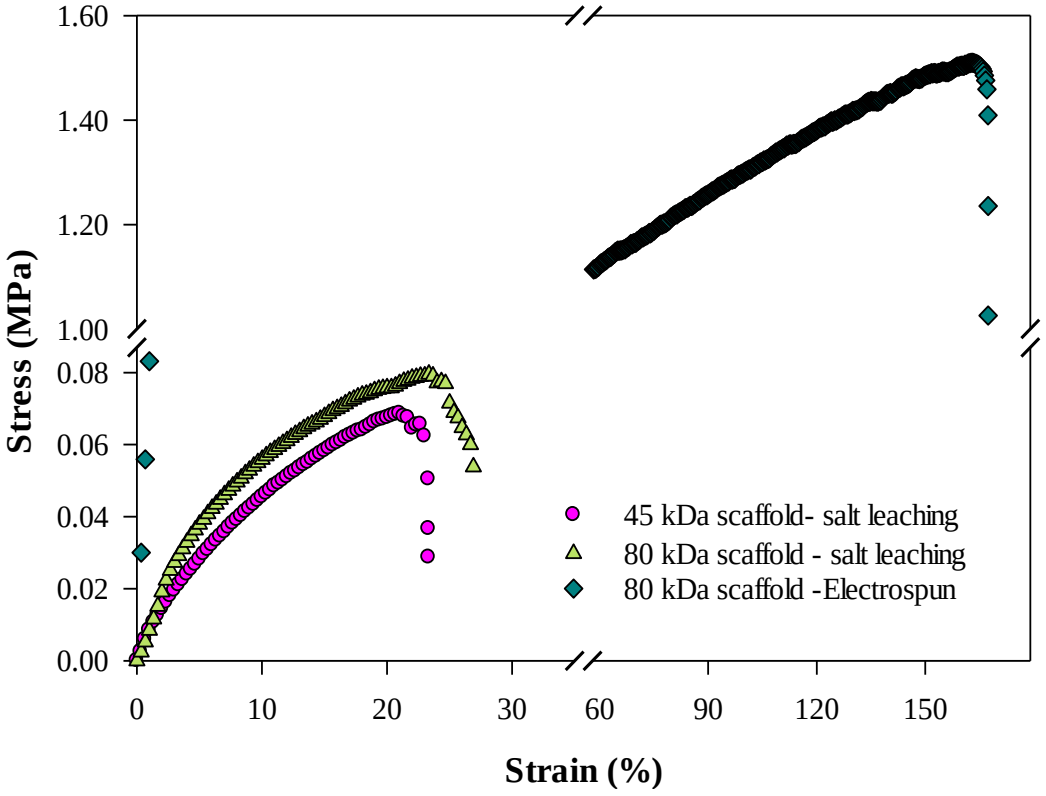

Figure 3.2.Stress-Strain behavior of scaffolds in hydrated conditions at 37°C.

3.3.3. Stress-relaxation behavior

Samples were subjected to five stages of ramp and hold tests to understand the stress relaxation behavior. All the scaffolds and films showed (**Figure 3.3**) a progressive increase in stress value for each stage. The salt leaching scaffolds accumulated up to 0.2 MPa stress at the end of five stages whereas the scaffold by electrospun technique accumulated up to 0.7 MPa stress for five stages, for the same amount of net strain. These values were comparable to that of other reports for electrospun fibers[30], although their tests were performed in dry at 37°C. This suggested that the effect of water on relaxation characteristics is minimal as PCL is hydrophobic material.

Nevertheless, comparison of the values by electrospun scaffolds to salt leached scaffolds showed enhanced relaxation in electrospun fibers. The accumulated stress in films was greater than 4.5 MPa, which is significantly higher for the same strain rate in five stages. Both 45 kDa and 80 kDa scaffolds were more elastic than films, attributed to the presence of pores. In general, 80 kDa structures had higher elasticity than 45 kDa structures, similar to uniaxial tensile testing.

In order to understand the relaxation behavior in different stages, all stages of each sample were plotted by translating the stress pattern for each stage to its origin which is shown in **Figure 3.4**. For 45kDa scaffolds by salt leaching technique and films the relaxation progressively decreased in subsequent stages. In 80 kDa scaffolds prepared by salt leaching technique there was no significance of effect of number of stages but there was a significant accumulation of stress in scaffolds by electrospun technique. The effect of stress accumulation was found to be more on films than scaffolds.

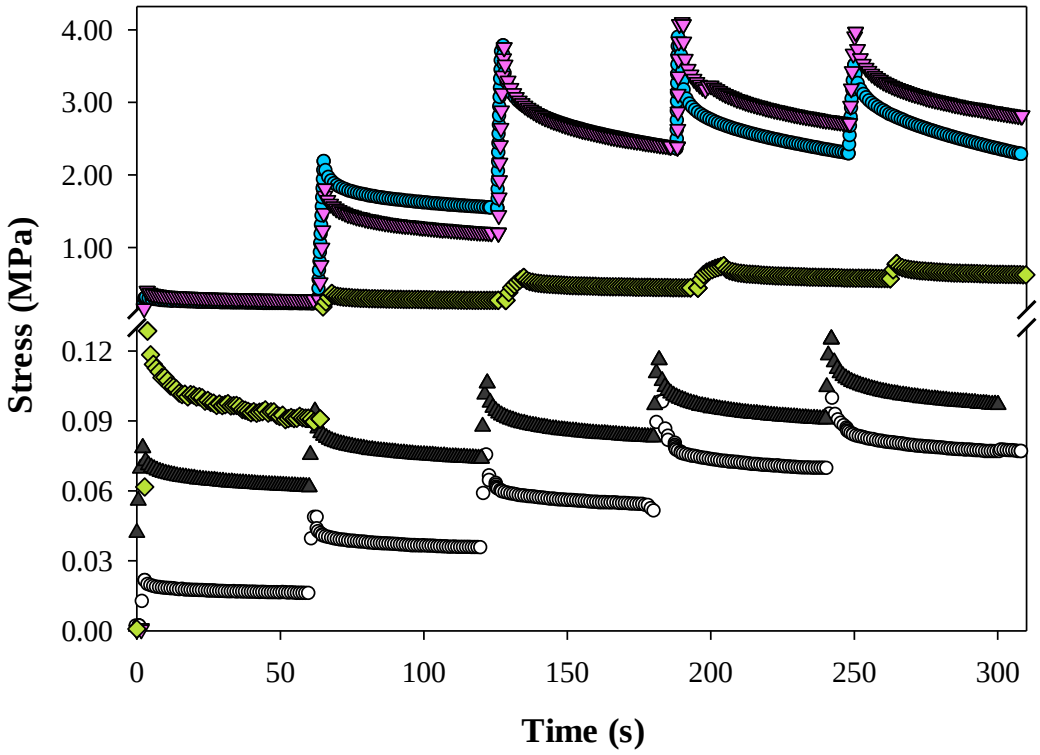

Figure 3.3.Dynamic behavior of 45 kDa and 80 kDa scaffolds and films with a strain rate of 1% s^{-1}. ○= 45kDa salt leached scaffolds; ▲ = 80 kDa salt leached scaffolds; ♦= 80 kDa electrospun scaffolds; ●= 45kDa air dried films; ▼=80 kDa air dried films

Samples were also analyzed by SEM after stress relaxation test to understand the changes in the material morphology (**Figure 3.1**). In both MW PCL salt leached scaffolds, no changes were observed in pore distribution in majority of the area except in few regions where pores appeared to orient in random directions. In electrospun scaffolds, largely no changes were observed in the distribution of fibers. This is unlike that reported for chitosan scaffolds, majority of the pores gets oriented in the direction of pull [24].

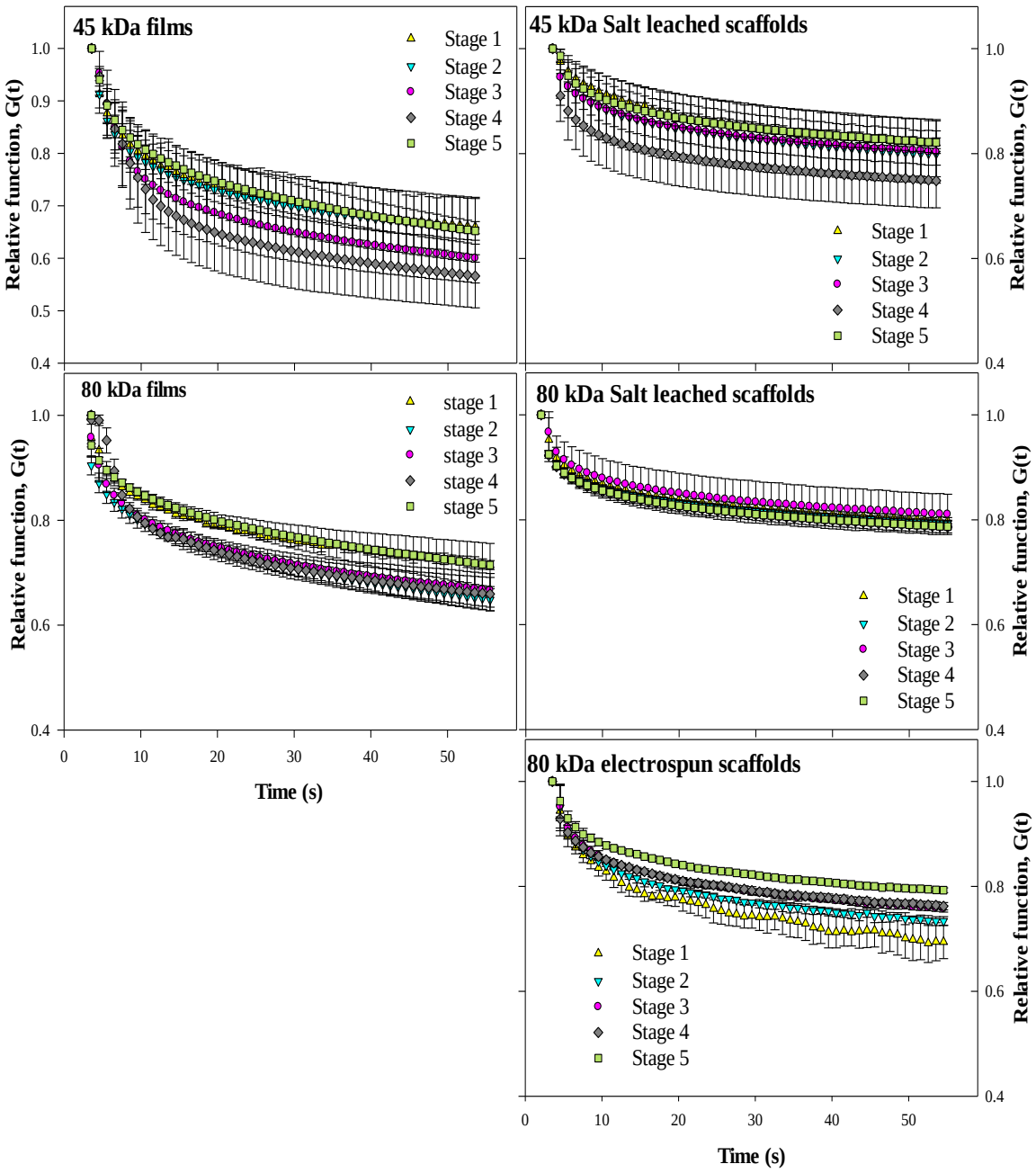

Figure 3.4. Relaxation behavior of scaffolds and films in different stages of ramp and hold tests. (a) 45 kDa Films (b) 45 kDa scaffolds- Salt leaching (c) 80 kDa Films (d) 80 kDa scaffolds- Salt leaching (e) 80 kDa scaffolds –Electrospun. Shown values are average of three samples and error bars correspond to standard deviations.

3.3.4. Alterations in relaxation behavior in the first stage

As the maximum stress for each sample was different, reduced relaxation functions G(t) was plotted by normalizing the relaxation portion of the data to the highest stress

experienced by each structure in the first stage. Further, to compare the results of 45 kDa films with different loading and relaxation time, which were pulled to 30% strain at the same strain rate of 1% s^{-1} by loading for 30s, the time axis was also normalized by dividing each time with 60 s which is the duration of each stage. From G(t) plots (**Figure 3.5**), the scaffolds prepared by salt leaching technique consistently showed less relaxation than films; only 15-20% of the stress is relaxed in each scaffold sample. 80 kDa scaffolds and films had a higher relaxation than 45 kDa scaffolds and films.

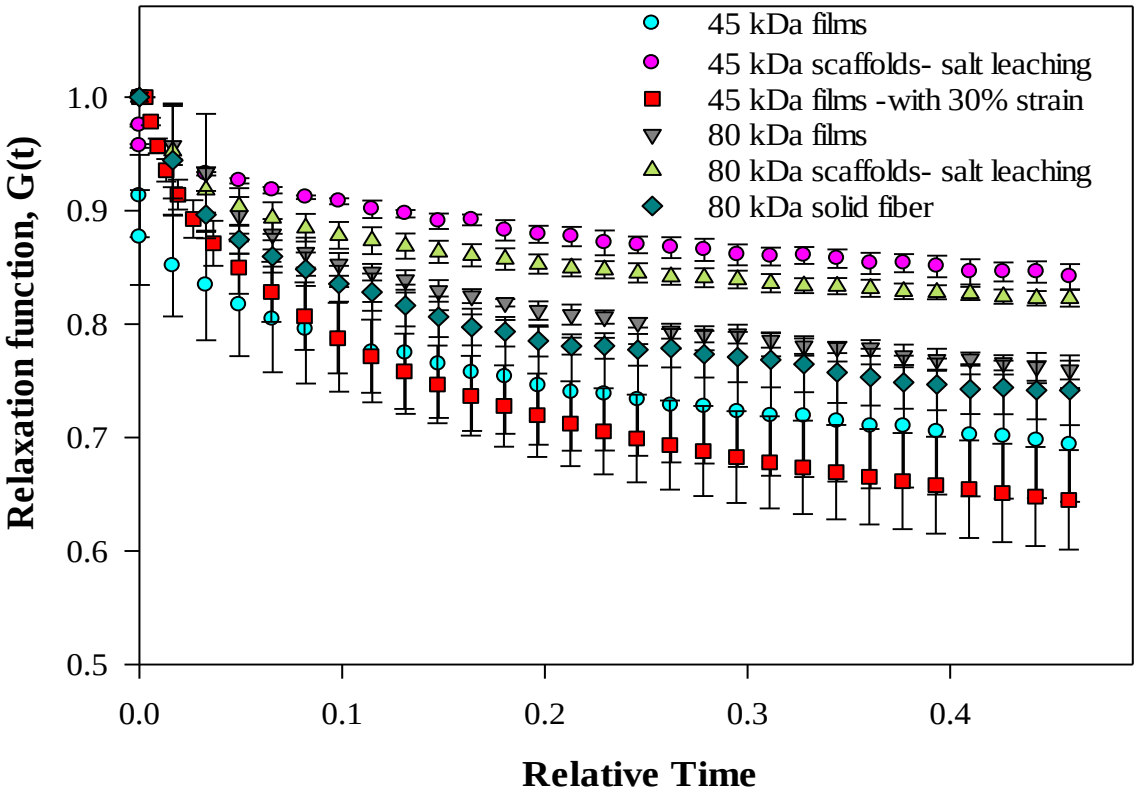

Figure 3.5.Normalized- relaxation function, G (t), plot of trends of first cycle of each strain rate. Shown values are average of three samples and error bars correspond to standard deviations.

80 kDa scaffolds prepared by electrospun technique showed the relaxation behavior similar to 80 kDa films. The difference in percentage of relaxations between the 45 kDa and 80 kDa scaffolds and films were similar. 45 kDa films with higher strain rate

showed higher relaxation in first stage but had a similar relaxation behavior at higher stages. This suggests that the polymer preconditioning occurs during the loading cycle. However, further experiments are necessary to better understand these behaviors.

3.4. SUMMARY AND DISCUSSION

This study focused on understanding the effect of scaffold processing of synthetic polymers on relaxation characteristics. Others have reported on the effect of pore architecture on dynamic mechanical properties [61]. The relaxation time, however, does not significantly affect relaxation behavior. From previous publications, the stress relaxation behavior plots were found to be different in the ramp phase for synthetic scaffolds, it was convex for synthetic scaffolds but it was concave for natural tissues like ligaments [30, 62]. The percentage of stress relaxed in PCL films in the first stage was similar to that of 50:50 poly-lactide-co-glycoside (PLGA) films [63]. However, the stress accumulation of PLGA films decreased in successive stages, leading to strain softening. This difference could be attributed to the fact that 50:50 PLGA is an amorphous polymer whereas PCL is semi crystalline. Compared to our previous study in the same condition, the stress relaxation trend and the value of stress accumulation were similar for both chloroform-casted and self-assembled PCL films despite their difference in MW. The relaxation behavior was different from that of chitosan and chitosan/gelatin [7] and also from small intestinal sub mucosa, a natural matrix with high amounts of type1 collagen dispersed with other matrix elements[63]. Chitosan scaffolds showed 90% relaxation property at the end of each stage but PCL scaffolds showed only 25% relaxation at the end of each stage, probably blending of both the polymers may give a better relaxation

property. PCL begins to creep when a constant force is applied above T_g, thereby affecting the degree of crystallinity. PCL scaffolds by salt leaching shows higher degree of crystallinity than scaffolds prepared from melting compression technique [64]. PCL films casted from tetrahydrofuran (THF) showed that the degree of crystallinity decreases for increase in solution concentration. But for the same MW PCL scaffolds show an increase in crystallinity for the increase in concentration. This property varies for porous structure from that of films due to the effect of densification that produces the pore collapse [65].

In summary, the results show that the porosity of scaffolds prepared by both techniques was approximately 80%. Thickness of electrospun scaffolds has an effect in relaxation characteristics, as thicker the scaffolds break stress and break strain of scaffolds decreased. PCL scaffolds by electrospun technique relaxes more than the scaffolds by salt leaching technique, however films relaxes more than that of scaffolds. High MW structures were more elastic than low MW structures. In both scaffolds and films there was a progressive increase in stress value for each stage in ramp and hold tests. Although the amount of loading was changed, 45 kDa films showed similar relaxation behavior which implies that the polymer preconditioning occurs during the loading cycle.

CHAPTER IV

CHITOSAN-BASED SCAFFOLD ANALYSIS

4.1. Chitosan and Blends

Chitosan is a second largest natural polymer which is a modified carbohydrate polymer derived from the chitin component present in the shells of crustacean, such as crab, shrimp, and cuttle fish. It has been widely explored in tissue engineering field due to its biocompatibility, biodegradability, antibacterial, and wound-healing activity and also used extensively in our research group. Although chitosan by nature is less soluble in water, chitosan scaffolds are popularly employed for replacement of tissues. Chitosan scaffolds have been successfully used in articular cartilage engineering due to its structural similarity with glycosaminoglycan (GAG) found in articular cartilage [66]. This has an high importance as this GAGs play a vital role in chondrocyte morphology, differentiation and function [17]. Mechanical properties of chitosan scaffolds have been characterized and analyzed. In addition, the relaxation characteristics of chitosan and chitosan-gelatin scaffolds prepared by freeze drying technique have also been evaluated [7]. Using microstructure changes after the ramp and hold experiments, pseudo component modeling was also reported. The modeling approach was validated using

cyclical property prediction and experimentation. However, the effect of processing them into porous scaffolds via freeze drying has not been evaluated by comparing the characteristics to films. The objective in this study was to compare the relaxation behavior of chitosan as scaffolds and films structures.

4.2. MATERIALS AND METHODS

4.2.1. Materials

Chitosan of low molecular weight (M_n = 800,000), gelatin type A (300 bloom) and phosphate buffer salts (sodium chloride, potassium chloride, potassium dihydrogen phosphate, Sodium Monohydrate Phosphate heptahydrate) were purchased from Sigma (St Louis, MO). Hydrochloric acid was purchased from Pharmco (Brookfield, CT) and ethanol from EM Science (Gibbstown, NJ).

4.2.2. Generation of films

Chitosan solutions of 2wt %/v concentration were prepared using 0.06 M hydrochloric acid. For chitosan-gelatin solution, equal amount of gelatin was added to the chitosan solution. Both chitosan (20 mL) and chitosan- gelatin solutions (20 mL) were casted into rectangular shaped films on Teflon sheets which was made using silicone glue and was air dried under laminar hood overnight.

4.2.3. Thickness of films

Thickness of each sample was determined before performing the mechanical testing on these samples. A thin strip of the samples were cut adjacent to those sample used for

testing. The cut strips were coiled carefully so that they can stand orthogonal to the field of view. Digital micrographs of these were obtained at various locations through an inverted microscope equipped with a CCD camera. These micrographs were quantified for the thickness using image analysis software (Sigma Scan Pro, SPSS Science, Chicago, IL). At least 3 to 4 images were analyzed per sample, and the calculated thicknesses were used for determining the stress values during tensile testing.

4.2.4. Mechanical testing

The films were cut into dimensions of 50 mm long and 10 mm wide and were washed with ethyl alcohol and rinsed in 0.1% NaOH to remove the hydrochloric acid from the films. All mechanical tests were conducted on an INSTRON 5542 machine (INSTRON, Canton, MA) using both chitosan and chitosan-gelatin rectangular films. Data were recorded using the associated Merlin (INSTRON) software. All tests were carried out in hydrate medium (phosphate buffer solution at Ph 7.4) at 37 ^{0}C. Each test was performed minimum of three times with different sample under same conditions.

Tensile test: Chitosan and chitosan-gelatin samples were set in between the cross-head and the speed of cross head was set to 10 mm min $^{-1}$ to determine break strain and stress.

Stress- relaxation: Stress- relaxation behavior of the samples was tested by conducting the ramp and hold experiment. Five successive ramp and hold cycles were made, with a constant strain rate of 1% s^{-1} (ramp) for 2 seconds followed by 58 seconds relaxation (hold). The cumulative strain limit was fixed 10% per ramp based on load limits determined from the tensile behavior of the films.

4.3. RESULTS

4.3.1. Structure Thickness

Thickness of the air dried chitosan films was found to be 0.087 (± 0.032) mm and that of chitosan-gelatin films were found to be 0.1123 (± 0.028) mm. Thickness was calculated for 3 samples and the average value was used as thickness in ramp and hold test.

4.3.2. Tensile testing

Uniaxial tensile testing was performed to set the load limits for performing ramp and hold tests so that tests would not exceed break stress or break strain. These results showed that chitosan films had a break stress of 0.5 MPa whereas chitosan gelatin films had 0.9 MPa (**Figure 4.1**). Both chitosan and chitosan-gelatin films had a break strain of 0.15-0.18 mm/mm. Since the break strain of both chitosan and chitosan gelatin films was around 15-18% strain the Young's modules was calculated for in the range up to 10% strain and was found to be 3.833 MPa and 5.733 MPa for chitosan and chitosan gelatin films respectively. The break stress was significantly lower for chitosan scaffolds and chitosan-gelatin scaffolds, which showed a break stress of 3 kPa [7]. The break strain for films were less relative to 25–30% break stress observed in scaffolds. Although the scaffolds had a different break strain, stress relaxation behavior of films was performed with the same strain rate of 1% s^{-1} that used for scaffolds [7].

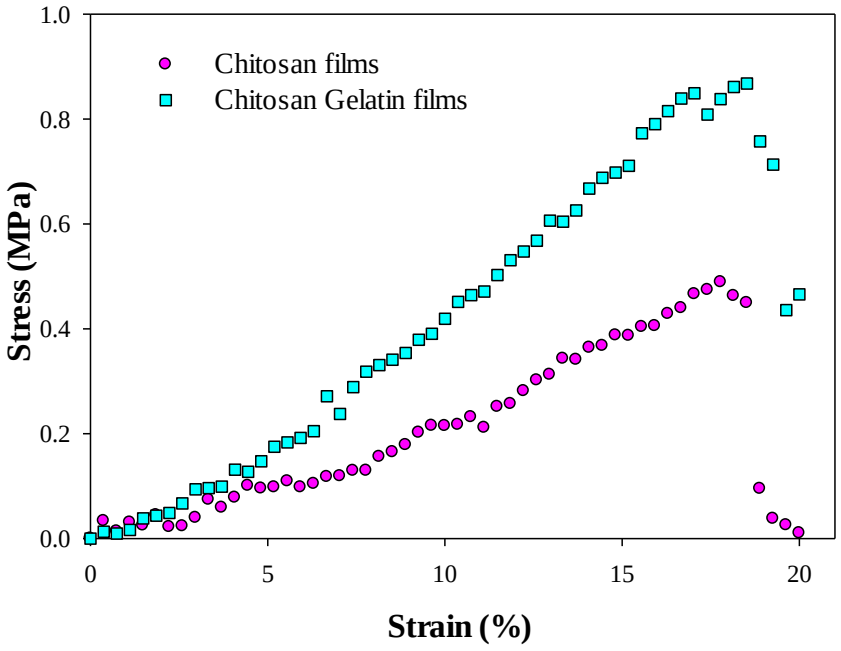

Figure. 4.1. Stress-Strain behavior of films in hydrated conditions at 37°C

4.3.3. Stress-relaxation behavior

Samples were subjected to five stages of ramp and hold tests to understand the stress relaxation behavior of chitosan films at constant tensile strain applied for a known time and then the samples were held for a certain time. Both chitosan and chitosan-gelatin films showed a progressive increase in stress value for each stage. Both chitosan and chitosan-gelatin films accumulated up to 0.24MPa stress at the end of five stages, for the same amount of net strain (**Figure 4.2**).

Chitosan films relaxed to the same extent as chitosan gelatin films but their trends in each stage varied. In order to understand the relaxation behavior at different stages within a sample, all stages were plotted by transforming the coordinates in each stage to the origin (**Figure 4.3**). Chitosan films in the first stage relaxed up to 70% and the relaxation reduced with each subsequent stage and the final stage relaxed up to 15%. This is unlike

the chitosan scaffolds, where no difference was observed in the amount of relaxation in different stages. In chitosan scaffolds, the stress relaxation was identical and was nearly 90% [7]. In chitosan-gelatin the films relaxed up to 80% in the first stage and the relaxation decreased for each stage progressively and the last three stages relax up to 20%. The relaxation in last three stages of chitosan gelatin films were nearly similar, the effect due to stages was very less. There was no significant difference in the relaxation behavior in the presence of gelatin in the scaffolds.

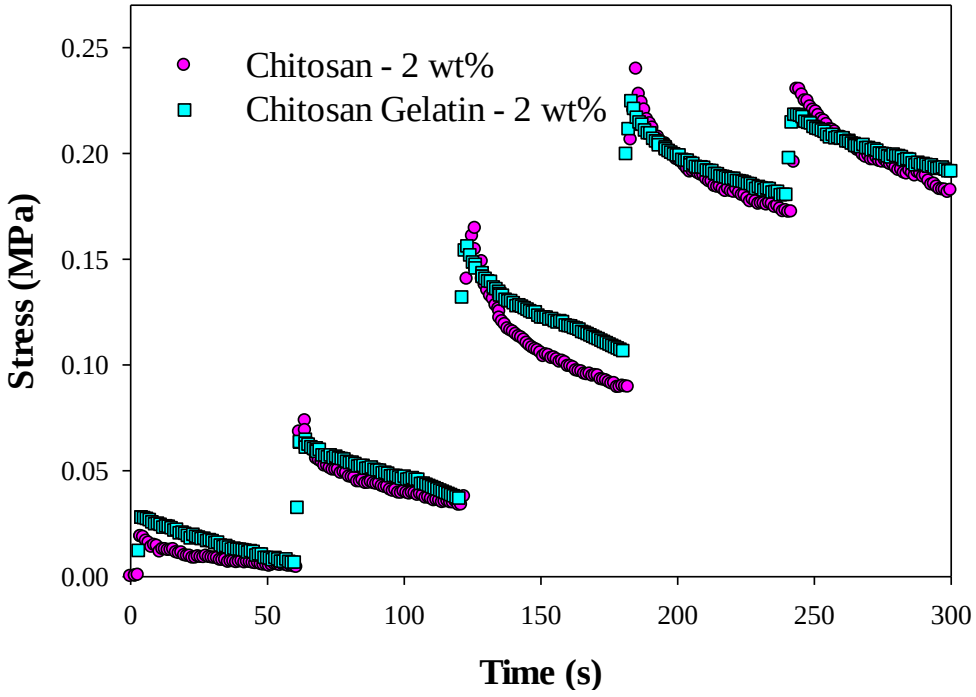

Figure.4.2. Dynamic behavior of chitosan and chitosan gelatin films with a strain rate of 1% s^{-1}.

As the maximum stress for each sample was different, reduced relaxation functions G(t) were plotted by normalizing the relaxation portion of the data to the highest stress experienced by each structure in the first stage. In addition, relaxation plots for chitosan and chitosan-gelatin scaffolds from a previous publication [7] were also plotted to assess

the effect of processing on chitosan samples comparison. These results showed (**Figure 4.4**) that there was a significant difference between scaffolds and films structures relaxation behavior.

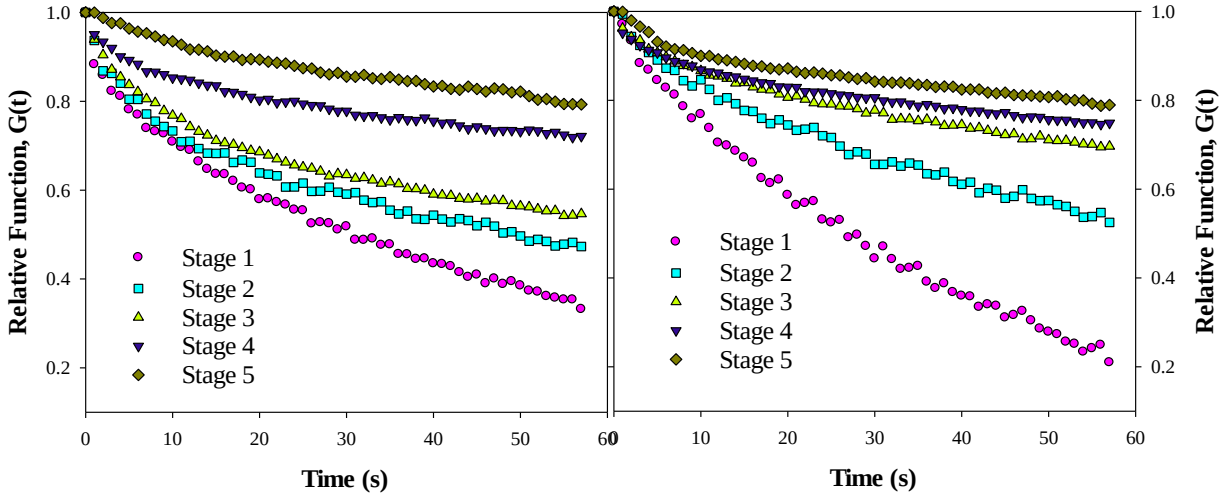

Figure.4.3. Relaxation behavior of films in different stages of ramp and hold tests. (a) Chitosan films (b) Chitosan gelatin films

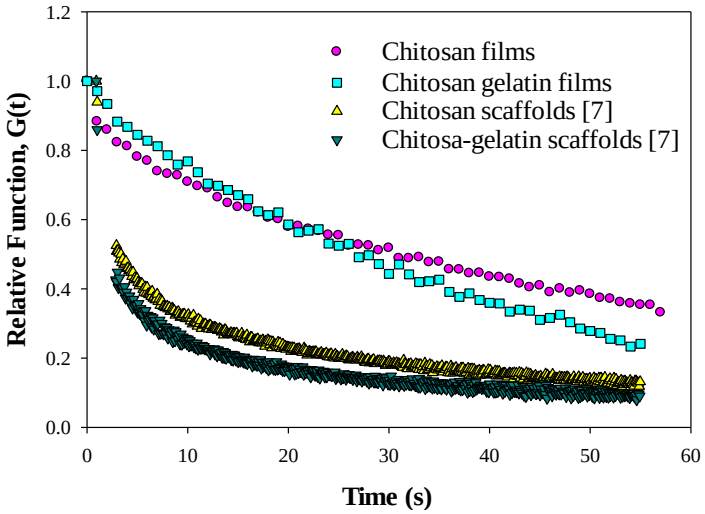

Figure. 4.4. Normalized- relaxation function, G (t), plot of trends of first cycle of films and scaffolds with 1% s^{-1} strain rate. Results for the scaffolds are from reference [7].

The scaffolds nearly showed an exponential decay in stress relaxation whereas the films showed nearly a linear relaxation during the hold time. Also, the films relaxed up to 70% whereas the scaffolds relaxed up to 85%. So in chitosan polymer scaffold structures relaxes more than film structures.

4.4. SUMMARY

In order to understand the effect of processing in chitosan, films formed by air drying technique were analyzed for stress relaxation behavior along with the previously published scaffolds results formed by freeze drying technique. Initial tensile tests indicated that the break strain for films was lower when compared to that of scaffolds. Hence, the ramp and hold test was carried out at reduced strain limit for films. Chitosan and chitosan–gelatin films relaxed up to 75% and 80% respectively in the first stage. The relaxation amount decreased for each stage and by the end of fifth stage chitosan films relaxed up to 15% and chitosan–gelatin films relaxes up to 20%. Staging had an effect on the relaxation behavior of films, as the film accumulates certain amount of stress within itself in each stage and relaxes lesser stress than the previous stage. This was true for both chitosan and PCL films structures. But in case of scaffolds the relaxation in first 10 seconds is higher than its relaxation in the following 40 seconds and the effect of staging in scaffolds is also lesser than in films.

CHAPTER V

MODELING

5.1. Viscoelastic modeling

Modeling viscoelastic behavior of scaffolds and films can help in monitoring the changes in stress-strain behavior of these scaffold placed in the body. The theory of quasi-linear viscoelasticity (QLV), has been widely used to model the viscoelastic response of soft tissues due to its ease and relatively limited number of material parameters to model the tissue behavior [67]. Other modeling techniques have also been evolved in the biomaterials to capture the viscoelastic behavior accurately. Previously our research group have reported on pseudo-component modeling approach for chitosan and chitosan-gelatin scaffolds [7]. This modeling approach was developed using combinations of four components which includes hyper-elastic spring, spring and dashpot, retain and reform components.

Hyper-elastic spring - the material would snap back to its original structure if external load was removed;

Spring and dashpot - this component doesn't account for any change in dimensions after the load is removed; do not relax the internal stress;

Retain - the material gets aligned in the stretched direction and relieves stress by setting to the new orientation;

Reform - In the elongated material, the polymer chains will arrange in original random orientation.

The basic equation used in deriving the model equations was the Hooke's law of elasticity where the stress (σ) and the applied strain (ε) is related as $\sigma_i = A_i(e^{B_i\varepsilon_i} - 1)$; in which A and B represents the parametric constants. Also, it is assumed that the viscoelastic pseudo-component undergoing internal material deformation are modeled of having their rate of internal stress relaxation in the order of 1, which at infinite time tends towards complete relaxation of zero stress. The relaxation model with no strain-rate induced stress is, $\tau_i \frac{d\sigma_i}{dt} + \sigma_i = 0; \sigma_i(t = 0) = \sigma_0$. The model was developed in Excel-VBA environment and the objective function was to reduce the sum of squared deviations (SSD) between the experimental and modeled stress values. $SSD = \Sigma(\sigma_{experimental} - \sigma_{model})^2$. The decision variable for reducing the SSD are A, B in hyper-elastic spring and A, B, τ for other pseudo components (spring and dashpot, Retain, Reform). Leapfrogging optimizer was employed in reducing the objective function [68].

Two composite models were developed (i) 5-parameter model: This structure had one hyper-elastic spring component (Parameters are $A_1$and B_1) in parallel with one pseudo-component (Parameters are A_2 , $B_2$and τ_2) (ii) 8-parameter model: This structure had one hyper-elastic spring component (Parameters are $A_1$and B_1)in parallel with two pseudo-components (Parameters are A_2 , B_2, τ_2, A_3 , $B_3$and τ_3).

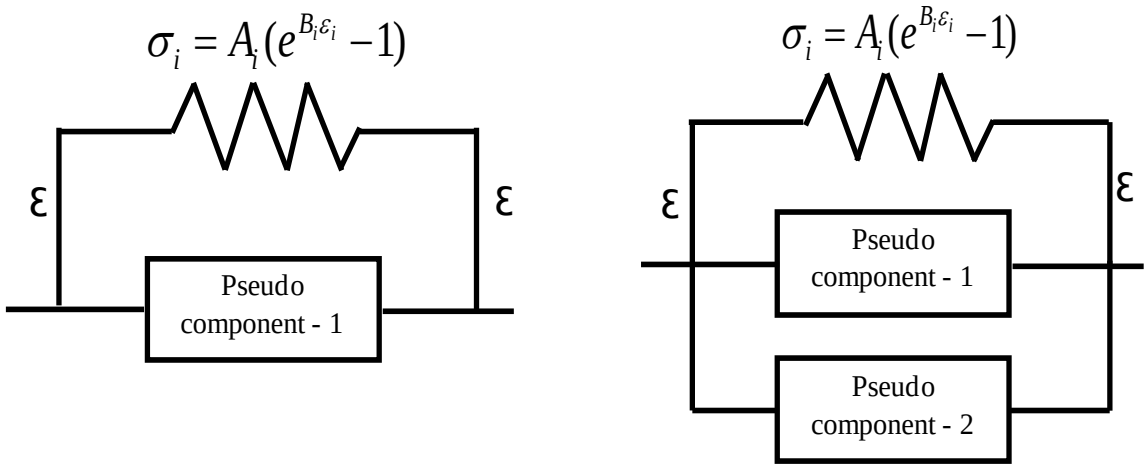

Figure 5.1. 5 and 8 parameter models with hyper elastic spring and appropriate pseudo components.

From previous studies the modeling results on chitosan and chitosan-gelatin scaffolds showed a suitable fit to the experimental data but the physical interpretation of eight parametric values were difficult as the values were distributed in all four coordinates (+/+, -/+, +/-, and -/-) with replicate experiments. The objective was to investigate the model adaptation to the relaxation characteristics of PCL scaffolds and also to understand the relation between the parametric values. So, the pseudo component modeling was performed for PCL salt leached scaffolds.

5.2. PSEUDO – COMPONENT MODELING

5.2.1. Modeling Approach

The modeling approach used in this study was similar to the previous study [7] and the detailed summary of the approach were described in the publication. In brief, six models with different combinations of pseudo component were developed and the macros were

written for six models in Visual Basic Applications, accessed through MS Excel. The six models developed were:

Composite Model 1: One hyper-elastic spring with two spring-and-dashpot components.

Composite Model 2: One hyper-elastic spring with two reform components.

Composite Model 3: One hyper-elastic spring with two retain components.

Composite Model 4: One hyper-elastic spring with one retain and one spring-and-dashpot component.

Composite Model 5: One hyper-elastic spring with one reform and one spring-and-dashpot component.

Composite Model 6: One hyper-elastic spring with one reform and one retain component.[7]

The experimental data containing ramp and relaxation parts for all five stages were exported to MS Excel and macros were run to obtain the parametric value that fits the experimental data. The Leapfrogging optimizer was employed in obtaining the parametric values with least SSD in each trail. The parametric values were sorted and the one with least SSD from 100 trials were taken to obtain the modeled stress values.

5.2.2. Modeling Chitosan films

For modeling chitosan scaffolds hyper elastic spring with retain-retain components were chosen as it had the least SSD among all other models [7] and also from the SEM images of scaffolds taken after the test, it shows that the material was oriented along the direction of pull which supports the combinations of components. Hence, similar components (hyper elastic spring with retain-retain) were used in modeling chitosan films. Averaged

stress values from 3 experiments performed using 3 different chitosan film prepared from same procedure were used for modeling. This was performed mainly to verify the flexibility of pseudo component modeling to film structures. These results showed in **Table 5.1 and Table 5.2**. In chitosan and chitosan gelatin scaffolds the SSD values from 8-parameter model were found to be lesser than the SSD values from 5-parameter model. Whereas in chitosan and chitosan gelatin films the SSD values (SSD for 5 stages of ramp and hold tests) for both the 5- and 8-parameter model were found be similar in the magnitude of 210- 240 kPa^2.

When modeled for 4 stages of ramp and hold tests of chitosan films the SSD values reduced from the magnitude of 200 kPa^2 to 25 kPa^2. By normalizing the SSD values to number of stages we get (200/5 = 40 kPa^2) 40 kPa^2 per stage; so for 4 stages (40*4 = 160 kPa^2) of experimental data we should get approximately get the SSD in the magnitude of 160 kPa^2. But the SSD value for 4 stages was found to be approximately 25 kPa^2 which explains that the decrease in SSD value is not due to the reduction in experimental data points. This is due to the fact that in first four stages the increase in stress values from each stage was approximately uniform whereas for the fifth cycle the increase in stress was much lesser than expected from the trend. So, when the model tries to fit for five stages we get a much higher SSD than when we fit for first four stages. This also indicates that the strain put on the material is at its yield point during its 5^{th} stage and may result in following new stress-strain mechanisms.

Chitosan films require less number of components for modeling which is verified from the model parameters. The parametric values of chitosan films shows that the values of third component parameters becomes approximately zero which explains that it doesn't

need the third component for modeling. Similarly, in chitosan-gelatin films, although it gives significant parametric values for the third component it ends up with same SSD value as that from the 5-parameter model.

Table. 5.1. Parameters and SSD values of five-parameter model for Chitosan

Chitosan	Scaffolds - 5 stages		Films - 5 stages		Films - 4 stages	
Parameter	Chitosan	Chitosan-Gel (CG)	Chitosan	Chitosan-Gel	Chitosan	Chitosan-Gel
A 1 (kPa)	12070.120	58401.237	197.457	212.745	37.100	18.241
B1	0.001	0.000	9346.222	7884.458	26536.23	33722.17
A2 (kPa)	14.115	36.161	9.555	39.378	3.115	48.120
B2	3.208	1.810	28453.64	16575.82	40040.67	20763.92
Tau2 (s)	6.012	4.418	14.953	9.869	36.280	16.018
SSD (kPa^2)	364.247	115.700	215.314	215.457	17.524	23.495

T able. 5.2. Parameters and SSD values of Eight-parameter model for Chitosan

Chitosan	Scaffolds - 5 stages		Films - 5 stages		Films - 4 stages	
Parameter	Chitosan	CG	Chitosan	CG	Chitosan	CG
A 1 (kPa)	-51.766	-4.689	220.890	212.745	39.158	-1.826
B1	-0.165	-4.174	8814.370	7884.458	25459.150	0.000
A2 (kPa)	7.385	-387111.43	3.961	209.854	3.115	43.402
B2	5.576	0.000	30597.300	1.018	45716.740	20449.626
Tau2 (s)	0.931	11.832	13725.500	0.000	24.515	18.698
A3 (kPa)	-16689.63	-1603328.58	-0.005	39.378	-0.002	19.303
B3	-0.002	0.000	0.000	16575.820	0.000	31793.208
Tau3 (s)	13.382	0.558	0.004	9.869	2.244	15676.061
SSD (kPa^2)	174.534	64.259	238.980	215.457	23.495	9.658

The plot comparing the experimental results with modeled results of chitosan and chitosan-gelatin scaffolds and films with strain rate of 1% s^{-1} for 2 s followed by 58 s hold per stage adding to accumulative strain of 10% for 5 stages has been shown in **Figure 5.2.**

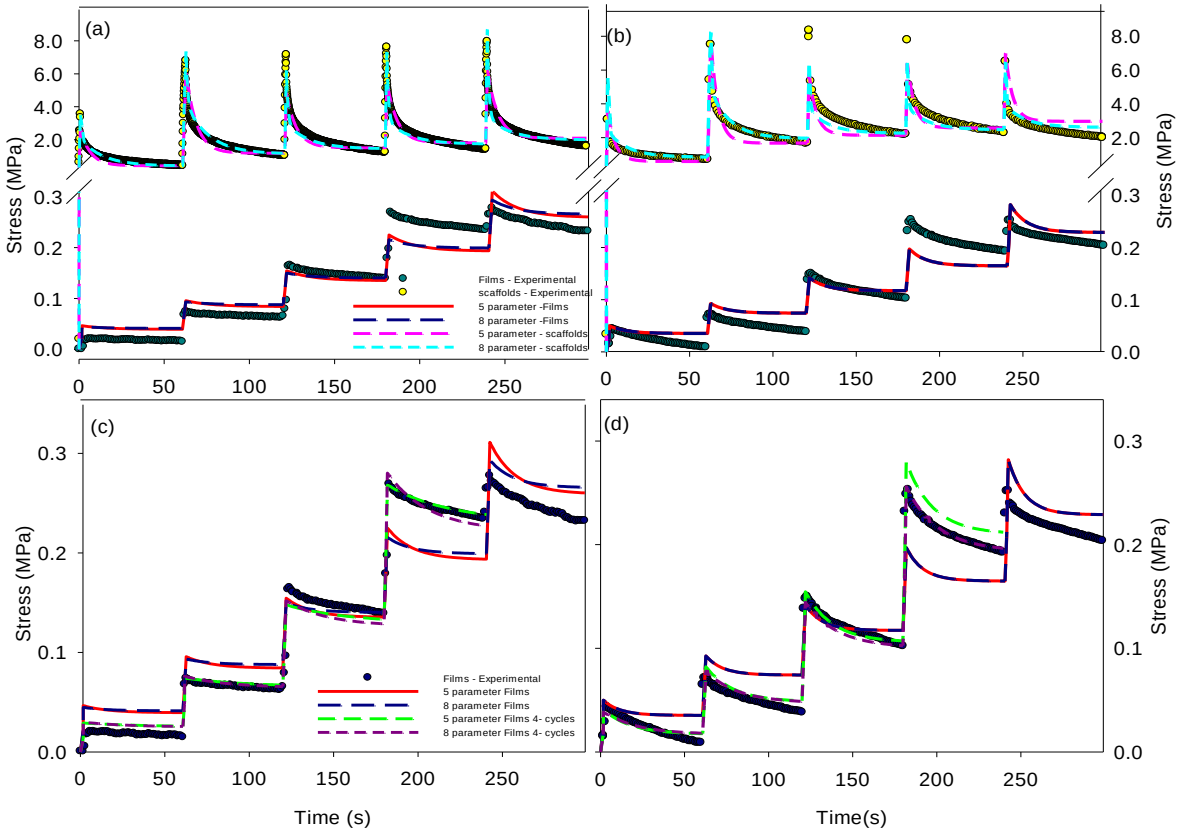

Figure 5.2. Experimental and 5 and 8- Parameter Model Plots (a) Chitosan Films and Scaffolds (b) Chitosan-Gelatin Films and Scaffolds (c) Chitosan films – different stages (d) Chitosan-Gelatin films – different stages

5.2.2 Modeling PCL Scaffolds and Films

Several combinations of were attempted to fit the averaged experimental results of 80 kDa salt leached PCL scaffolds (**Table 5.3).** SSD values for the model RET-REF with components hyper-elastic spring, retain, reform gives a least SSD value. Even though model SD-REF with components hyper-elastic spring, spring and dashpot and reform gives the SSD value in the same order of magnitude but the plot shown in **Figure 5.3** shows RET-REF model follows the experimental trend better than SD-REF model. Also SEM images (**Figure 3.1)** of scaffolds taken before and after relaxation test show that the PCL scaffolds, after relaxation tests are found to be arranged in a random orientation. In few regions they get aligned to the direction of pull.

Table.5.3. Parameters and SSD values of 80 kDa salt leached scaffolds from different models

Parameters	RET-RET	SD-RET	SD-REF	RET-REF
A 1 (kPa)	-4757.220	-102.843	-47.757	-1075.720
B1	-23.071	-8571.850	-220000000.000	-829.304
A2 (kPa)	-412.911	-54.825	-17.343	-61.278
B2	-3271.410	-458854.000	-420040.000	-70725.500
Tau2 (s)	568.041	334.856	3.155	312.991
A3 (kPa)	14.292	-4269.140	-2198.800	-15.129
B3	19976.960	-336.706	-418.917	-789996.000
Tau3 (s)	3.917	1.759	403.261	3.291
SSD (kPa^2)	31.518	157.573	7.677	2.409

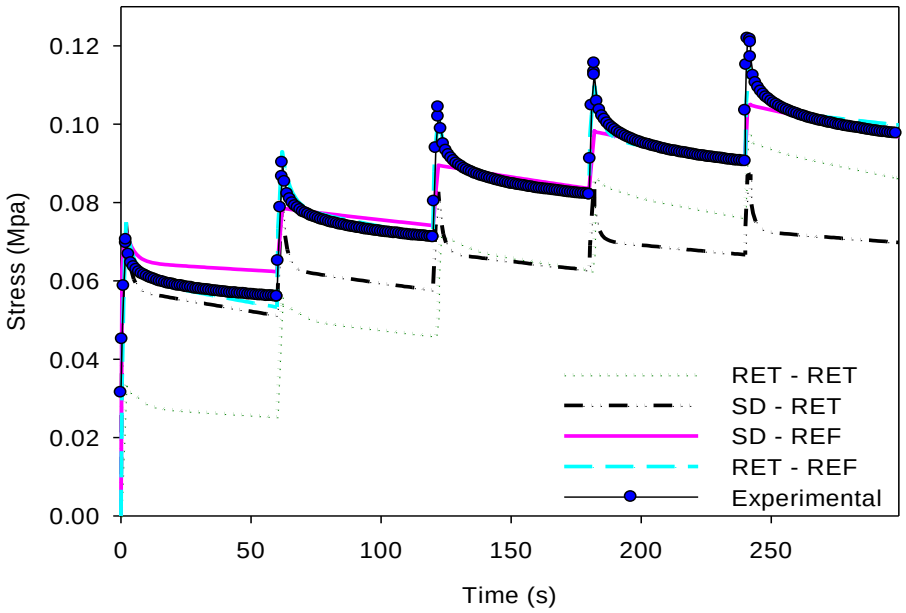

Figure 5.3. Experimental and Different model 8- Parameter model Plots of 80 kDa salt leached scaffolds

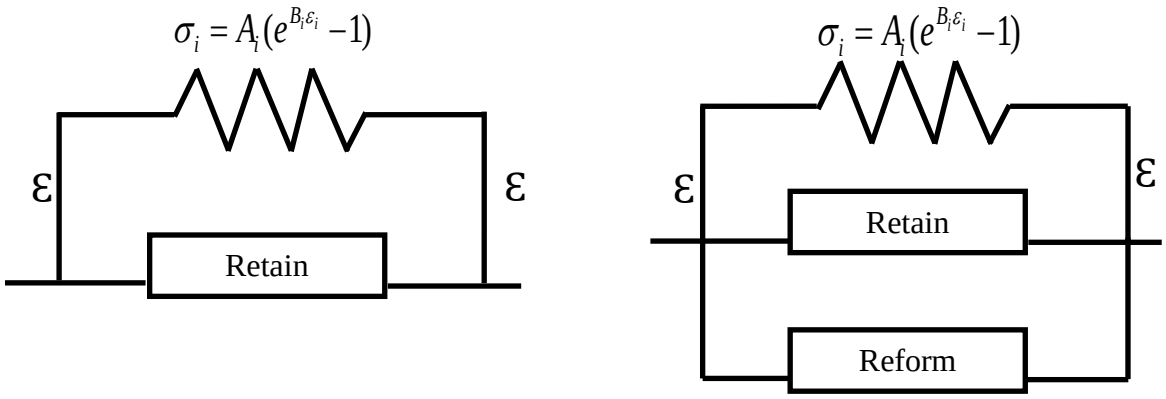

Figure 5.4. 5 parameter model and 8 parameter for PCL modeling

Hence, for modeling other PCL scaffolds and films structures, RET-REF model with pseudo components hyper-elastic spring, retain and reform were chosen for obtaining the

model stress values. Similar relaxation tests were carried out for PCL films as that of scaffolds with the cumulative strain of 10% for 5 stages in ramp and hold tests. Pseudo component modeling was performed for 45 kDa and 80kDa salt leached scaffolds and air dried films. The Parametric values of both scaffolds and films of 5- and 8-parameter model are shown in Table-5.4and 5.5 respectively

Table.5.4. Parameters and SSD values of five-parameter model for PCL

PCL	Scaffolds – 5 stages		Films – 5 stages	
Parameters	45 kDa	80 kDa	45 kDa	80 kDa
A 1 (kPa)	-197.310	-37.520	-3280.300	-6219.400
B1	-5934.000	-800000000.00	-13384.00	-7809.800
A2 (kPa)	3.880	3374.410	1631.680	1085.800
B2	28193.900	373.490	15949.300	17472.500
Tau2 (s)	6.520	249.490	4.940	7.280
SSD(kPa^2)	8.800	4.690	36164.200	43344.200

Table.5.5. Parameters and SSD values of eight-parameter model for PCL

PCL	Scaffolds - 5 stages		Films - 5 stages	
Parameters	45 kDa	80 kDa	45 kDa	80 kDa
A 1 (kPa)	-129.580	-1075.700	-3300.490	-6753.370
B1	-6255.000	-829.300	-12958.530	-6966.320
A2 (kPa)	2.130	-61.280	589.280	31.680
B2	33653.100	-70726.000	24917.570	43800.360
Tau2 (s)	3.130	312.990	0.880	0.440
A3 (kPa)	2052.510	-15.130	0.070	0.010
B3	185.710	-789996.000	461397.120	568938.970
Tau3 (s)	521.110	3.290	7.340	6.410
SSD(kPa^2)	10.820	2.410	36164.330	36703.110

The plots of experimental and modeled plots of both PCL scaffolds and films were shown in **Figure 5.5**. Both the 5 and 8 parameter model was able to follow the relaxation trends of scaffolds as the increase in stress values for each stage was uniform. So, the SSD values for both the 45 and 80 kDa scaffolds were in the magnitude of 10 kPa^2, but in both the 5- and 8-parameter model the 80 kDa scaffolds had the lesser SSD in the magnitude of 5 kPa^2 when comparing it with 45 kDa scaffolds which had the SSD values in the magnitude of 10 kPa^2. In case of both 45 kDa and 80 kDa films the SSD values were in the magnitude of 37000 kPa^2 which is much higher than that of scaffolds. This is due to the fact that in films the increase in amount of stress in its third stage varies from the trend that was followed in the previous and successive stages. As the model tries to fit this increased stress in third stage it results in higher SSD from the experimental results.

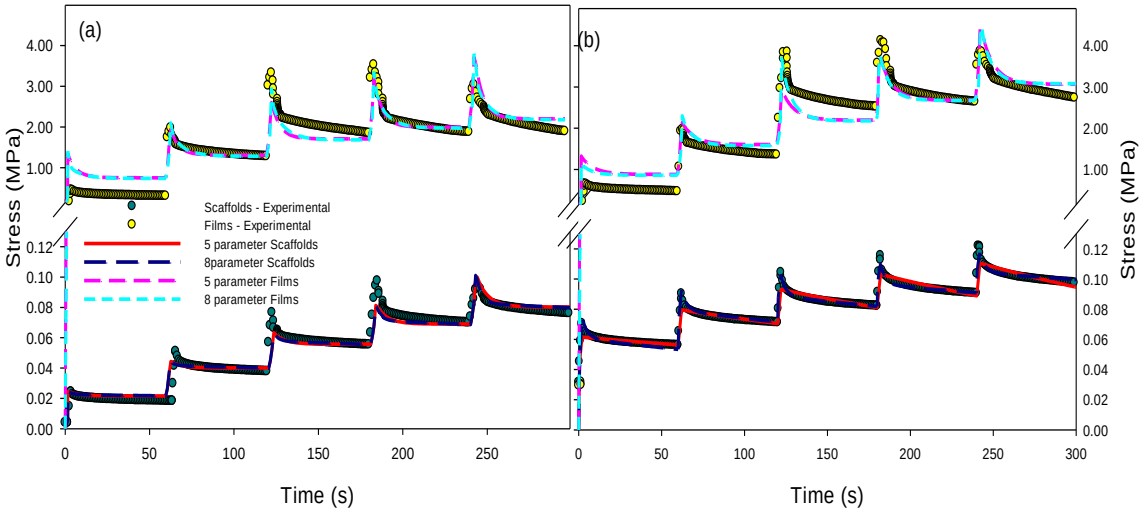

Figure 5.5.Experimental and 5 and 8- Parameter Model Plots (a) 45 kDa scaffolds and films (b) 80 kDa scaffolds and films

5.3. MODEL VALIDATION: Cyclic tests

Cyclic tests are conducted to understand the behavior of these scaffolds in performing actions like walking, cycling and others. As in these activities the strain rate is repeated, the strain gets backs to initial stage and again reaches the same strain rate.

Mechanical testing

All tests were conducted in a physiological conditions (phosphate buffer solution at pH 7.4 at 37^0C) using INSTRON 5542 machine (INSTRON, Canton, MA) and a custom-built environmental chamber. The 80 kDa salt leached, electrospun scaffolds and films were cut into dimensions of 50 mm long and 10 mm wide and set between the crossheads. Each test was performed 3 or more times using samples from different preparations.

Cyclical tests: Samples were cycled at a cross head speed of 50 mm/min (0.864 mm/s) with the load limits between 0.056N to 0.016N. The cyclical behavior was determined using the associated software, Merlin (INSTRON Canton, MA). The samples were stretched and relaxed toward the original length repeatedly between two preset loads for five cycles. The pseudo component modeling can be validated by using the parametric values from stress relaxation test to predict the cyclic behavior in scaffolds and films. The responses of scaffolds and films stresses were in the limit between 0.01MPa and 0.035MPa. The strain range of scaffolds was between 0.1 to 0.5% and for the films it was between 0.2 to 0.7%. The relaxation tests were carried out in the strain region of 0 to 10% with stress range of 0 to 0.3 MPa and the parametric values from these range was used in predicting the cyclic behavior with the strain rate of 0 to 0.5% and stress limit from 0 to 0.04 MPa. Although predicting the cyclic behavior in a very narrow region of

strain limit compared to that of relaxation tests, the model was able to capture the cyclical trend in scaffolds, but was not able to predict that well for films. For this reason pseudo component modeling was carried out only for the first stage of relaxation behavior where the strain limit was 2% and the parameters from these regions was used to predict the cyclic behavior. The 8-parameter model was able to predict and capture the trends of 80 kDa salt leached scaffolds of winding and relaxing with increase in strain limit for the cyclic tests, but it was not able to reach the maximum stress reached in experiments. Model predictions from 2% of strain limit showed a better fit to experimental data than the model predictions from 10% strain rate.

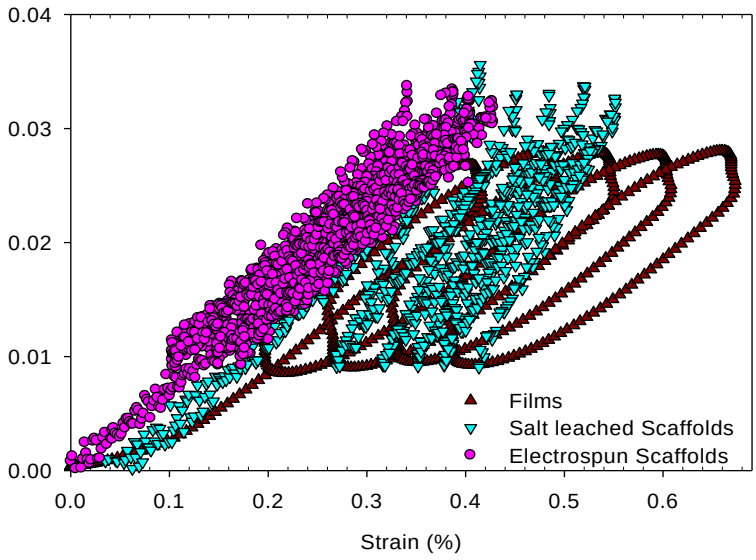

Figure 5.6. Cyclical experiments on 80 kDa Films, Salt leached and Electrospun Scaffolds

The responses of scaffolds and films stresses were in the limit between 0.01MPa and 0.035MPa. The strain range of scaffolds was between 0.1 to 0.5% and for the films it was between 0.2 to 0.7%. The relaxation tests were carried out in the strain region of 0 to 10% with stress range of 0 to 0.3 MPa and the parametric values from these range was

used in predicting the cyclic behavior with the strain rate of 0 to 0.5% and stress limit from 0 to 0.04 MPa. Although predicting the cyclic behavior in a very narrow region of strain limit compared to that of relaxation tests, the model was able to capture the cyclical trend in scaffolds, but was not able to predict that well for films. For this reason pseudo component modeling was carried out only for the first stage of relaxation behavior where the strain limit was 2% and the parameters from these regions was used to predict the cyclic behavior. The 8-parameter model was able to predict and capture the trends of 80 kDa salt leached scaffolds of winding and relaxing with increase in strain limit for the cyclic tests, but it was not able to reach the maximum stress reached in experiments. Model predictions from 2% of strain limit showed a better fit to experimental data than the model predictions from 10% strain rate.

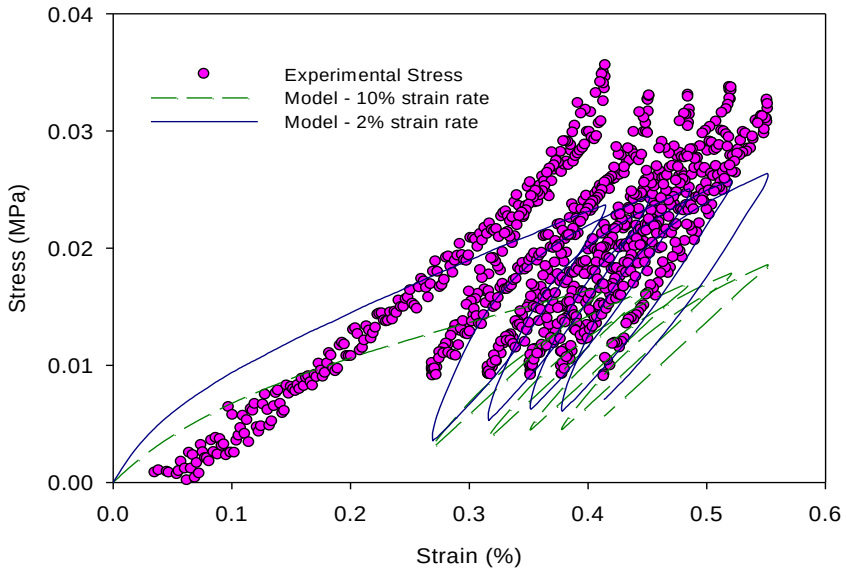

Figure 5.7. Experimental and 8-Parameter Model Cyclical Plots for 80 kDa PCL salt leached scaffolds with 10% and 2% strain range.

In 80 kDa electrospun scaffolds the model was able to reach the maximum stress and capture the trend of cyclic tests as the five stages in experimental plot was clustered together, and the model was also able to predict the same and shows a closed clustered trend. The 5-parameter model was not able to predict the cyclic behavior of these scaffolds. Both 80 kDa PCL scaffolds prepared by different technique shows varied cyclic behavior with the same strain limit, this shows that there is an effect of processing techniques in viscoelastic behavior.

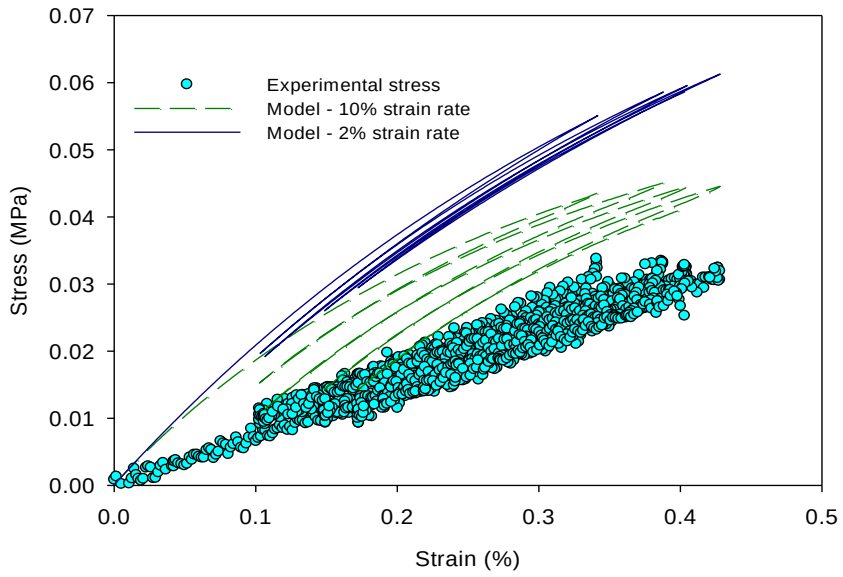

Figure 5.8. Experimental and 8-Parameter Model Cyclical Plots for 80 kDa PCL electrospun scaffolds with 10% and 2% strain range.

In case of 80 kDa films it shows a varied behavior from that of scaffolds. The hysteresis curves were observed in films going up to the strain of 0.7%. The model prediction from 10% strain rate was not able to capture the trend and resulted in stress values in the range of 0.3 MPa similar to that from ramp and hold tests. But the model parameters from 2%

strain rate were able to follow the trend and give the modeled stress values in the range of 0 to 0.02MPa. In cyclical behavior model predictions the cycle repeats itself without forming any hysteresis curves, so that the different cycles are not visible in the plots. However the models predictions were much better for scaffold structures than for film structures.

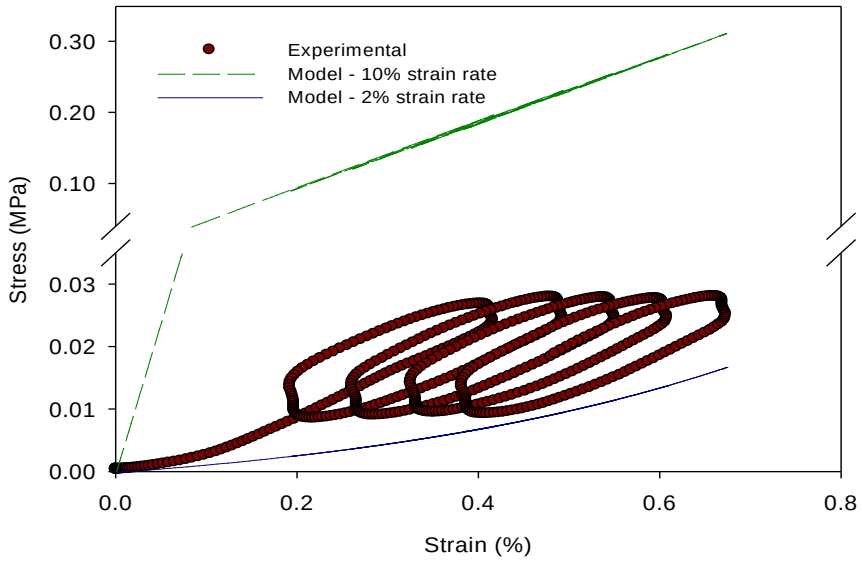

Figure 5.9. Experimental and 8-Parameter Model Cyclical Plots for 80 kDa PCL films with 10% and 2% strain range.

5.3.1. ALTERNATIONS IN CYCLICAL BEHAVIOR OF FILMS

In PCL film structures when the experiment was carried out between different load limits of 0.036N to 0.010N, 0.056N to 0.016N and 17.5N to 5N it shows a varied behavior. As the load limits gets higher the hysteresis curves disappears and gives a repeatable cycle. In case of natural tissues the cyclical characteristics show hysteresis curve for all cycles. As the load limits gets higher the strain and stress limits also increases.

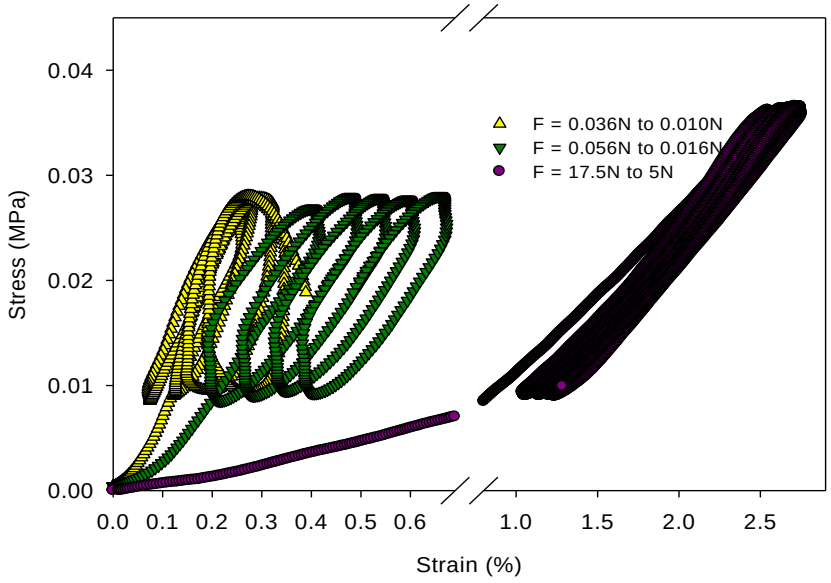

Figure 5.10. Cyclical experiments on 80 kDa PCL films with varied load limits

5.4. SUMMARY

Viscoelastic constitutive models have been extensively developed in the mechanical engineering, materials science, and bioengineering literature. Also, modeling the material experimental viscoelastic behavior can help in monitoring the changes in the stress-strain behavior of the scaffold that is placed in the body [69]. As the modeling for chitosan scaffolds has been already established, I started modeling chitosan film structures using similar components used for scaffolds. The results showed that the chitosan films do not need the third component for modeling the relaxation behavior. By modeling for 4 stages of chitosan films the SSD values decreased than expected explaining that the films reaches the yield point after 8% strain. With this background the modeling was extended to PCL scaffolds and films. Various combinations of models have been tried and the combinations of the pseudo component were chosen based on the

model with gives a least SSD with capability to capture the trend. Also the orientation of material after the relaxation tests was analyzed in choosing the components which gives more realistic approach to pseudo component modeling. As the increase in stress for each stage was approximately uniform in PCL scaffolds; the model was able to capture the trends giving the SSD values in the magnitude of 10 kPa^2. In case of PCL films the increase in stress value at third stage was much higher than the increase in stress values at previous and subsequent stages. So, when the model tries to fit the third stage it ends in high value of SSD values in the magnitude of 37000 kPa^2. In validating the model cyclical tests were performed within the load limits of 0.056N to 0.016N which resulted in a narrow strain range of 0 to 0.4% and the model parameters from 0 to 10% range was able to capture the trend of cyclic behavior even in that narrow region.

CHAPTER VI

CONCLUSIONS AND RECOMMENDATIONS

Specific aim was to analyze the effect of processing scaffolds on viscoelastic properties.

PCL scaffolds synthesized by salt leaching technique and electrospun technique were characterized using SEM analysis where both high and low MW scaffolds were found to be approximately 80% porous. High MW scaffolds were 82% porous and low MW scaffolds were 81% porous. Thickness of the scaffolds was measured using digital vernier caliper, where the salt leached scaffolds were found to be thicker than electrospun scaffolds for same amount of solution used for preparing the scaffolds. Electrospun scaffold thickness has an effect in relaxation behavior, thicker the scaffolds the break stress of the scaffolds decreased. Thickness of films were calculated using the images taken from light microscopy and was used in ramp and hold experiments. Electrospun scaffolds possessed much higher break strain and break stress than salt leached scaffolds. Films possess higher break strain and stress than electrospun scaffolds. In G(t) plots where five stages of each scaffolds were plotted showed similar relaxation trends; the

first stage relaxed more whereas the successive stages followed the trend but relaxed lesser than the first stage. In comparing the G(t) plot for first stage scaffolds synthesized by electrospun technique relaxes more than that of salt leached scaffolds, however films relaxes more than that of scaffolds. In both scaffolds and films there was a progressive increase in stress value for each stage in ramp and hold tests. Although the amount of loading was changed, 45 kDa films showed similar relaxation behavior which implies that the polymer preconditioning occurs during the loading cycle.

Specific aim was to understand the relaxation behavior in natural polymer- chitosan and synthetic polymer- PCL as different structures (films and scaffolds) Chitosan scaffolds relax up to 85% whereas films relax up to 70%, which implies that scaffolds relax more than films in natural polymer chitosan. In case of synthetic polymer PCL films relaxes up to 30% whereas electrospun scaffolds relaxes up to 20% and salt leached scaffolds relaxes up to 12%, which implies that in PCL films relaxes more scaffolds. Thus natural polymer chitosan and synthetic polymer PCL show difference in relaxation behavior trends as different structures. Effect of staging is dominant in both chitosan, PCL films than scaffolds.

Specific aim was to investigate the model adaptation of viscoelastic behavior to synthetic polymer scaffolds and to explore on the flexibility of pseudo component modeling on films. Pseudo component modeling was previously carried out for chitosan scaffolds with that background I have extended it to chitosan films initially. It was able to predict the ramp and hold behavior of films and the sum of squared deviation (SSD) between the experimental and modeled values were found to approximately same for both chitosan and chitosan-gelatin films for 5 stages. But the SSD was greatly reduced for 4 stages

when compared to SSD values of 5 stages this may be due to the fact that at 10% strain the films would have followed new stress-strain mechanisms. In 5-parameter model chitosan films possessed lesser SSD than 8-parameter model whereas in chitosan scaffolds 8-parameter model possessed lesser SSD than 5-parameter model. In case of synthetic polymer PCL the 5 and 8 parameter model was able to adapt to the trend of scaffolds behavior and gave a SSD in the magnitude of 10 kPa^2 whereas it was not able to follow the trend in films which resulted SSD values in the magnitude of 37000 kPa^2. Model was validated by conducting cyclical test for PCL scaffolds and films, the parametric values were able to predict the cyclical trends.

Recommendations:

1. As the eventual target of this project is to set back the synthesized scaffolds along with populated cells into native environment. The viscoelastic properties of scaffolds without cells have been studied and this could be extended to analyzing the viscoelastic properties along with cells in it. Cells suitable for specific application (Example. liver cells, endothelial cells, muscle cells) should be made to populate and fed on to scaffolds. After the cells populate scaffolds and synthesize the extracellular matrix elements, uniaxial tensile testing needs to be carried out under physiological conditions to calculate the break stress and strain values to set the strain limit for ramp and hold tests. By conducting the ramp and hold test we can understand whether the scaffolds with cells shows any varied behavior. These experiments can also be carried out for different conditions such as varied media for cell culture, varied growth period for cells to populate.

2. In reality during our standing posture the tissues in the lower regions of our body are exposed to continuous compressive force, so evaluating the viscoelastic behavior for compressive forces also becomes important. Experiments were carried out for tensile stress relaxation behavior; it can be extended to similar uniaxial compressive test and creep tests under physiological conditions to calculate break stress and break strain. Compressive tests are carried out by setting a constant strain rate until the break strain is reached whereas creep tests are carried out under constant compression and the strain rate will be recorded at specific time intervals. By these tests we will be able to understand the viscoelastic behavior of scaffolds for compressive forces.

3. Pseudo component modeling has to be explored furthermore, to get a relationship between the parametric values to porous architecture and relaxation behavior. We have parametric values in all quadrants and also the time constant come to be a huge number due to which we were not able to make out a physical relation between parameters and relaxation behavior. In order to get a correlation I tried modeling the relaxation characteristics by restricting the parameters to only positive quadrant, scaffolds resulted in parameters of acceptable range but the model was not able to follow the relaxation trends, whereas in films it was able to follow the trend but resulted in very high SSD. Recently modeling using energy density function has become popular. In models using energy density function the stress tensor is decomposed into initial and non-equilibrium parts which end up in a simple numerical integration terms simpler than other nonlinear modeling techniques and easy implementation of associated algorithms into other modeling codes. So by using energy density function which is the product of stress and strain within pseudo component modeling can be used to model the viscoelastic behavior.

4. The cyclical tests are carried out by setting the load but it also be performed by setting within the required strain limit. By which we can compare the behavior at different strain range and also will be significant in predicting the cyclical behavior by using the parameters from a particular strain range.

5. In synthesizing the salt leached scaffolds a quick test has to conduct to verify that all the salt has been dissolved from the scaffolds. This can be done by measuring the difference in weight of air dried scaffolds with salt and the weight of scaffolds after dissolving the salt from the scaffolds.

6. In pseudo component modeling the films may give a least SSD value for different combinations of components so predicting the components for modeling films should also be done rather than choosing the similar components from that used for scaffolds.

REFERENCES

1. Hutmacher, D.W., *Scaffolds in tissue engineering bone and cartilage.* Biomaterials, 2000. 21(24): p. 2529-2543.
2. Gobin, A.S., V.E. Froude, and A.B. Mathur, *Structural and mechanical characteristics of silk fibroin and chitosan blend scaffolds for tissue regeneration.* Journal of Biomedical Materials Research Part A, 2005. 74A(3): p. 465-473.
3. Mathieu, L.M., et al., *Architecture and properties of anisotropic polymer composite scaffolds for bone tissue engineering.* Biomaterials, 2006. 27(6): p. 905-916.
4. Hou, Q., D.W. Grijpma, and J. Feijen, *Porous polymeric structures for tissue engineering prepared by a coagulation, compression moulding and salt leaching technique.* Biomaterials, 2003. 24(11): p. 1937-1947.
5. Hong, J.K. and S.V. Madihally, *Three-dimensional scaffold of electrosprayed fibers with large pore size for tissue regeneration.* Acta Biomater, 2010. 6(12): p. 4734-42.
6. Pok, S.W., K.N. Wallace, and S.V. Madihally, *In vitro characterization of polycaprolactone matrices generated in aqueous media.* Acta Biomaterialia, 2010. 6(3): p. 1061-1068.
7. Ratakonda, S., et al., *Assessing viscoelastic properties of chitosan scaffolds and validation with cyclical tests.* Acta Biomaterialia, 2012. 8(4): p. 1566-1575.
8. E. Niklason, L. and R. S. Langer, *Advances in tissue engineering of blood vessels and other tissues.* Transplant Immunology, 1997. 5(4): p. 303-306.
9. Oh, S.H., et al., *In vitro and in vivo characteristics of PCL scaffolds with pore size gradient fabricated by a centrifugation method.* Biomaterials, 2007. 28(9): p. 1664-1671.
10. Hile, D.D., et al., *Active growth factor delivery from poly(d,l-lactide-co-glycolide) foams prepared in supercritical CO2.* Journal of Controlled Release, 2000. 66(2–3): p. 177-185.
11. Chandra, R.R., Renu, *Biodegradable polymers* PROG POLYM SCI (OXFORD). , 1998. 23(7): p. 12731335.
12. Adhikari, P.A.G.a.R., *BIODEGRADABLE SYNTHETIC POLYMERS FOR TISSUE ENGINEERING.* European cells and materials, 2003. 5: p. 1-16.
13. Athanasiou, K.A., et al., *Orthopaedic applications for PLA-PGA biodegradable polymers.* Arthroscopy: The Journal of Arthroscopic & Related Surgery, 1998. 14(7): p. 726-737.
14. Woodruff, M.A. and D.W. Hutmacher, *The return of a forgotten polymer—Polycaprolactone in the 21st century.* Progress in Polymer Science, 2010. 35(10): p. 1217-1256.

15. Sarasam, A. and S.V. Madihally, *Characterization of chitosan–polycaprolactone blends for tissue engineering applications.* Biomaterials, 2005. **26**(27): p. 5500-5508.
16. Madihally, S.V. and H.W.T. Matthew, *Porous chitosan scaffolds for tissue engineering.* Biomaterials, 1999. **20**(12): p. 1133-1142.
17. Di Martino, A., M. Sittinger, and M.V. Risbud, *Chitosan: A versatile biopolymer for orthopaedic tissue-engineering.* Biomaterials, 2005. **26**(30): p. 5983-5990.
18. Kim, I.-Y., et al., *Chitosan and its derivatives for tissue engineering applications.* Biotechnology Advances, 2008. **26**(1): p. 1-21.
19. Keenan, T.R., *Gelatin*. Encyclopedia Of Polymer Science and Technology Vol. 6. 2002 John Wiley & Sons, Inc. 311-324.
20. Yin, Y., et al., *Preparation and characterization of macroporous chitosan–gelatin/β-tricalcium phosphate composite scaffolds for bone tissue engineering.* Journal of Biomedical Materials Research Part A, 2003. **67**(3): p. 844-855.
21. Kang, H.-W., Y. Tabata, and Y. Ikada, *Fabrication of porous gelatin scaffolds for tissue engineering.* Biomaterials, 1999. **20**(14): p. 1339-1344.
22. Zhen Zhao Guo, H.L., Wei Cheng Guan, Bo Xue, Chang Ren Zhou, *Preparation of Mineralized Electrospun PCL/Gelatin Scaffolds via Double Diffusion System.* Key Engineering Materials 2012. **512-515**: p. 1740-1745.
23. Tiaw, K.S., et al., *Processing Methods of Ultrathin Poly(ε-caprolactone) Films for Tissue Engineering Applications.* Biomacromolecules, 2007. **8**(3): p. 807-816.
24. Qingpu Hou, D.W.G., Jan Feijen, *Preparation of Porous Poly(e-caprolactone) Structures.* Macromol. Rapid Commun, 2002,. **4**(23): p. 247- 252.
25. Huang, Y.O., Stella; Siewe, Mbonda; Moshfeghian, Aliakbar; Madihally, Sundararajan V, *In vitro characterization of chitosan–gelatin scaffolds for tissue engineering.* Biomaterials, 2005. **26**(36): p. 7616-7627.
26. Gerçek, I., R.S. Tığ lı, and M. Gümüşderelioğ lu, *A novel scaffold based on formation and agglomeration of PCL microbeads by freeze-drying.* Journal of Biomedical Materials Research Part A, 2008. **86A**(4): p. 1012-1022.
27. Ma, P.X., *Scaffolds for tissue fabrication.* Materials Today, 2004. **7**(5): p. 30-40.
28. Hong, J.K. and S.V. Madihally, *Next generation of electrosprayed fibers for tissue regeneration.* Tissue Eng Part B Rev, 2011. **17**(2): p. 125-42.
29. Liang, D., B.S. Hsiao, and B. Chu, *Functional electrospun nanofibrous scaffolds for biomedical applications.* Advanced Drug Delivery Reviews, 2007. **59**(14): p. 1392-1412.
30. Duling, R., et al., *Mechanical Characterization of Electrospun Polycaprolactone (PCL): A Potential Scaffold for Tissue Engineering.* Journal of Biomechanical Engineering, 2008. **130**(1).
31. Yang, S., et al., *The design of scaffolds for use in tissue engineering. Part I. Traditional factors.* Tissue engineering, 2001. **7**(6): p. 679-689.
32. Lu, X.L., et al., *Study on the shape memory effects of poly(l-lactide-co-ε-caprolactone) biodegradable polymers.* Journal of Materials Science: Materials in Medicine, 2008. **19**(1): p. 395-399.
33. Jamison, C.E., R.D. Marangoni, and A.A. Glaser, *Viscoelastic properties of soft tissue by discrete model characterization.* J Biomech, 1968. **1**(1): p. 33-46.

34. Lanir, Y., *Constitutive equations for fibrous connective tissues.* J Biomech, 1983. **16**(1): p. 1-12.
35. Craiem D, *Fractional-order viscoelasticity applied to describe uniaxial stress relaxation of human arteries.* Phys Med Biol, 2008. **53**(17).
36. Defrate L.E and G. Li, *The prediction of stress-relaxation of ligaments and tendons using the quasi-linear viscoelastic model.* Biomech Model Mechanobiol, 2007. **6**(4).
37. Nekouzadeh, A., et al.,, *A simplified approach to quasi-linear viscoelastic modeling.* Journal of Biomechanics, 2007. **40**(14).
38. YC Fung, *Elasticity of soft tissues in simple elongation.* Am J Physiol, 1967. **213**(6): p. 1532-1544.
39. Purslow, P.P., T.J. Wess, and D.W. Hukins, *Collagen orientation and molecular spacing during creep and stress-relaxation in soft connective tissues.* The Journal of Experimental Biology, 1998. **201**(1): p. 135-42.
40. Abramowitch, S.D. and S.L. Woo, *An improved method to analyze the stress relaxation of ligaments following a finite ramp time based on the quasi-linear viscoelastic theory.* J Biomech Eng, 2004. **126**(1): p. 92-7.
41. Defrate, L.E. and G. Li, *The prediction of stress-relaxation of ligaments and tendons using the quasi-linear viscoelastic model.* Biomech Model Mechanobiol, 2007. **6**(4): p. 245-51.
42. Doehring, T.C., E.O. Carew, and I. Vesely, *The effect of strain rate on the viscoelastic response of aortic valve tissue: a direct-fit approach.* Ann Biomed Eng, 2004. **32**(2): p. 223-32.
43. Funk, J.R., et al., *Linear and quasi-linear viscoelastic characterization of ankle ligaments.* J Biomech Eng, 2000. **122**(1): p. 15-22.
44. Haslach, H.W., Jr., *Nonlinear viscoelastic, thermodynamically consistent, models for biological soft tissue.* Biomech Model Mechanobiol, 2005. **3**(3): p. 172-89.
45. Funk JR, H.G., Crandall JR, Pilkey WD, *Linear and quasi-linear viscoelastic characterization of ankle ligaments.* Journal of Biomechanical Engineering, 2000. **122**(1): p. 15-22.
46. Shazly, T.M., et al., *Viscoelastic adhesive mechanics of aldehyde-mediated soft tissue sealants.* Biomaterials, 2008. **29**(35): p. 4584-4591.
47. Toms, S.R., et al., *Quasi-linear viscoelastic behavior of the human periodontal ligament.* Journal of Biomechanics, 2002. **35**(10): p. 1411-1415.
48. Craiem, D., et al., *Fractional-order viscoelasticity applied to describe uniaxial stress relaxation of human arteries.* Phys Med Biol, 2008. **53**(17): p. 4543-54.
49. Boyce, B.L., et al., *Stress-controlled viscoelastic tensile response of bovine cornea.* J Biomech, 2007. **40**(11): p. 2367-76.
50. Bates, J.T., *A Recruitment Model of Quasi-Linear Power-Law Stress Adaptation in Lung Tissue.* Annals of Biomedical Engineering, 2007. **35**(7): p. 1165-1174.
51. Peña, E., J.A. Peña, and M. Doblaré, *On modelling nonlinear viscoelastic effects in ligaments.* Journal of Biomechanics, 2008. **41**(12): p. 2659-2666.
52. Haslach, H., Jr., *Nonlinear viscoelastic, thermodynamically consistent, models for biological soft tissue.* Biomechanics and Modeling in Mechanobiology, 2005. **3**(3): p. 172-189.

53. Wang, J.L., et al., *Development and validation of a viscoelastic finite element model of an L2/L3 motion segment.* Theoretical and Applied Fracture Mechanics, 1997. **28**(1): p. 81-93.
54. Jeffrey A. Weiss, J.C.G., Krista M.Quapp. *Material models for the study of soft tissue mechanics*. in *Pelvic and lower extremity injuries*. 1995.
55. Heo, S.J., et al., *Fabrication and characterization of novel nano- and micro-HA/PCL composite scaffolds using a modified rapid prototyping process.* J Biomed Mater Res A, 2009. **89**(1): p. 108-16.
56. Gercek, I., R.S. Tigli, and M. Gumusderelioglu, *A novel scaffold based on formation and agglomeration of PCL microbeads by freeze-drying.* J Biomed Mater Res A, 2008. **86**(4): p. 1012-22.
57. Draghi, L., et al., *Microspheres leaching for scaffold porosity control.* Journal of Materials Science: Materials in Medicine, 2005. **16**(12): p. 1093-1097.
58. Sill, T.J. and H.A. von Recum, *Electrospinning: Applications in drug delivery and tissue engineering.* Biomaterials, 2008. **29**(13): p. 1989-2006.
59. Lannutti, J., et al., *Electrospinning for tissue engineering scaffolds.* Materials Science and Engineering: C, 2007. **27**(3): p. 504-509.
60. Raghavan, D., et al., *Physical characteristics of small intestinal submucosa scaffolds are location-dependent.* J Biomed Mater Res A, 2005. **73**(1): p. 90-6.
61. Moroni, L., J.R. de Wijn, and C.A. van Blitterswijk, *3D fiber-deposited scaffolds for tissue engineering: influence of pores geometry and architecture on dynamic mechanical properties.* Biomaterials, 2006. **27**(7): p. 974-85.
62. Wang, C.C.B., C.T. Hung, and V.C. Mow, *An analysis of the effects of depth-dependent aggregate modulus on articular cartilage stress-relaxation behavior in compression.* Journal of Biomechanics, 2001. **34**(1): p. 75-84.
63. Mirani, R.D., et al., *The stress relaxation characteristics of composite matrices etched to produce nanoscale surface features.* Biomaterials, 2009. **30**(5): p. 703-710.
64. Barbanti, S.H., C.A.C. Zavaglia, and E.A.d.R. Duek, *Effect of salt leaching on PCL and PLGA(50/50) resorbable scaffolds.* Materials Research, 2008. **11**: p. 75-80.
65. Más Estellés, J., et al., *Physical characterization of polycaprolactone scaffolds.* Journal of Materials Science: Materials in Medicine, 2008. **19**(1): p. 189-195.
66. Temenoff, J.S. and A.G. Mikos, *Review: tissue engineering for regeneration of articular cartilage.* Biomaterials, 2000. **21**(5): p. 431-440.
67. Bischoff, J., *Reduced Parameter Formulation for Incorporating Fiber Level Viscoelasticity into Tissue Level Biomechanical Models.* Annals of Biomedical Engineering, 2006. **34**(7): p. 1164-1172.
68. Rhinehart, R.R., M. Su, and U. Manimegalai-Sridhar, *Leapfrogging and synoptic Leapfrogging: A new optimization approach.* Computers & Chemical Engineering, 2012. **40**(0): p. 67-81.
69. Meyers and Chawla, *"Mechanical Behavior of Materials.* 1999: p. 98-103.

VITA

Vijayalakshmi Sethuraman

Candidate for the Degree of

Master of Science

Thesis: VISCOELASTIC MODELING OF STRESS RELAXATION BEHAVIOR IN BIODEGRADABLE POLYMERS

Major Field: Chemical Engineering

Biographical:

Education:

- Completed the requirements for the Master of Science in Chemical Engineering at Oklahoma State University, Stillwater, Oklahoma in May, 2013.

- Completed the requirements for the Bachelor of technology in Chemical Engineering at Sri Sivasubramaniya Nadar College of Engineering, Anna University, Tamil Nadu, India in 2011 in Year.

Experience:

- Research Assistant, Laboratory for Molecular Bioengineering, OSU, Jan 2012- Dec 2012

- Teaching Assistant, Introduction to Thermodynamics course, OSU, Jan 2012- Dec 2012

- Teaching Assistant, Process Modeling course, OSU, Aug 2012- Dec 2012.

Professional Memberships:

- Omega Chi Epsilon, OSU Chapter.

- International Society of Automation (ISA), OSU Chapter.

- Indian Institute of Chemical Engineers (IIChE), SSN student Chapter.